Chapter 2 of

Flow in Collapsible Tubes and Past Other Highly Compliant Boundaries

Editors: P.W. Carpenter & T.J. Pedley

To be published by Kluwer.

Chapter 2

FLOWS IN DEFORMABLE TUBES AND CHANNELS
THEORETICAL MODELS AND BIOLOGICAL APPLICATIONS

M. HEIL
Department of Mathematics, University of Manchester,
Oxford Road, Manchester M13 9PL, UK

O.E. JENSEN
School of Mathematical Sciences, University of Nottingham,
University Park, Nottingham NG7 2RD, UK

Abstract

This chapter gives an overview of the main physiological applications of collapsible tube flows and reviews the major theoretical and computational developments of the past twenty-five years, ranging from lumped-parameter models to three-dimensional Navier–Stokes simulations. We also discuss some of the significant questions that, despite substantial progress, still remain open.

1. Introduction

Many fluid-conveying vessels in the human body are highly elastic and deform substantially in response to the traction (pressure and viscous stress) that the fluid exerts on them. The study of flows in elastic vessels is therefore of considerable interest in many biomechanicad biomedical applications. It also presents an interesting and extremely challenging fluid-mechanical problem in its own right. Experimental studies of flow in collapsible tubes, described in more detail in Chapter 3, show that the interaction between the finite-Reynolds-number internal flow and large deformations of the tube wall can cause the development of large-amplitude self-excited oscillations. Many distinct modes of oscillation have been observed experimentally. Understanding fully the mechanisms driving these oscillations remains a major research goal.

A completely rational theoretical description of flow in collapsible tubes would have to be based on the unsteady 3D Navier-Stokes equations, coupled to the equations of large-displacement shell theory. The numerical solution of this problem would require enormous computational resources, and would yield limited (but of course very valuable) insights into the underlying physics. Much theoretical work on flow in collapsible tubes has therefore concentrated on the development and analysis of simpler models, obtained, for example, by reducing the spatial dimension of the problem. Such simplified models invariably involve a number of *ad hoc* assumptions whose validity must be critically assessed as better models or more detailed experimental data become available.

The problem of flow in collapsible tubes has many obvious similarities to the problem of flow past compliant surfaces and coatings, which is reviewed in other Chapters in this volume. However, there are a few important differences between these problems. First, collapsible tube experiments are performed with finite-length elastic tubes whose upstream and downstream ends are held open. The inertia and resistance of the fluid in the supporting rigid tubes have an important influence on the system's overall dynamics; conversely, most (but not all) theoretical studies of flow past compliant coatings are based on infinite domains. Second, self-excited oscillations in collapsible tubes tend to have large amplitude and can develop from steady states in which the tube is strongly deformed, and in which the viscous pressure drop along the tube is significant; conversely, most stability analyses of flows past compliant coatings are based on perturbations of an initially uniform, undeformed state. Third, self-excited oscillations in collapsible tubes do not always require the presence of wall inertia, whereas most flutter-type analyses consider systems in which wall inertia is significant.

It is the aim of this Chapter to provide a review of previous theoretical

and computational analyses of flows in collapsible tubes (earlier review articles on the subject were written by Shapiro 1977, Kamm & Pedley 1989, Grotberg 1994 and Pedley & Luo 1998), to identify the current state of the art in the field, and to outline some open research problems. The Chapter includes brief summaries of relevant talks presented at the IUTAM Symposium. Since many of these talks contained unpublished work, we have included references to papers which, at the time of writing, are in press, under review or even in preparation.

The structure of this Chapter is as follows: Section 2 provides an overview of the major biological applications of collapsible tube flow. Section 3 introduces the model problem considered in most theoretical analyses and discusses its relation to typical laboratory experiments. Sections 4–6 discuss successively 1D, 2D and 3D models of flow in collapsible tubes. Finally, Section 7 provides a brief summary and some suggestions for future work.

2. Biological Background

The propagation of the pulse wave through the arterial system is a well-known and well-understood example of a physiological flow in which wall elasticity plays an important role. One-dimensional models, based on an inviscid description of the fluid dynamics, coupled to a simple description of the wall mechanics, are able to explain satisfactorily many features of this problem (see e.g. McDonald 1974, Lighthill 1975, Pedley 1980). The analysis of pulse-wave propagation is facilitated by the fact that under normal conditions the arteries are subject to a positive transmural (internal minus external) pressure and therefore remain inflated and relatively stiff throughout the pulse cycle. There are, however, many examples of fluid-conveying vessels that are subject to negative (compressive) transmural pressures, which cause the vessels to buckle and collapse non-axisymmetrically. Buckled vessels are very flexible and even small changes in fluid pressure can induce large changes of their cross-sectional area. This leads to a strong interaction between fluid and solid mechanics, which gives rise to many intriguing phenomena, including flow limitation and the propensity to develop large-amplitude self-excited oscillations.

Physiological examples of collapsible tubes are numerous, as are corresponding models, so the following list of topics is far from complete but hopefully reasonably representative. In the cardiovascular system, first of all, spontaneous collapse can occur in veins above the heart and outside the skull (due to hydrostatic reduction of blood pressure). This is particularly important in subjects with long necks, such as giraffes (see Pedley *et al.* 1996). Flow-induced collapse of blood vessels is believed to play a role in the auto-regulation of blood supply to many internal organs; see Rod-

bard & Takacs (1966) and Rodbard (1966). Dynamic flow-induced collapse of blood vessels downstream of atherosclerotic stenoses has been proposed as a mechanism of plaque rupture, which can lead to vessel occlusion distally, with potentially serious consequences (Binns & Ku 1989; Ku 1997). Blood vessels can also collapse as a result of external compression. Coronary blood vessels collapse during systole (see e.g. Gregg & Fisher 1963), and collapsible-tube models have been used to understand how compression mediates their delivery of blood to the myocardium (e.g. Guiot *et al.* 1990). Active compression of veins in the lower limbs is used successfully as a therapy to prevent deep-vein thrombosis; see e.g. Kamm (1982) and Olson *et al.* (1982). Both veins and arteries also collapse during sphygmomanometry, when an inflatable cuff is placed around the upper arm to measure blood pressure.

During micturition, the urethra behaves like a passive collapsible tube (e.g. Griffiths 1969, 1971), which can exhibit flow limitation effects. In contrast the ureter, and a number of other deformable muscular vessels in the body (particularly in the gut), transport fluid by active peristaltic pumping, a process which couples fluid, solid and muscle mechanics (e.g. Carew & Pedley 1997) in a manner that is only beginning to be properly understood.

Air flow in the lung is strongly affected by the elasticity of the airways. For instance during forced expiration, contraction of the expiratory muscles increases the pleural pressure that drives air out of the peripheral airways. If the pleural pressure increases beyond a critical level, it can initiate the collapse of the proximal airways. The reduction of their cross-sectional area increases the local fluid velocity. The Bernoulli effect, which then reduces the internal fluid pressure, leads to a further increase in compression. This mechanism causes an increasingly strong collapse of the airways and results in so-called flow limitation and possibly 'negative effort dependence,' whereby an increase in expiratory effort (at a given lung volume) beyond a certain level can lead to a reduction in expiratory flow rate.

Self-excited oscillations of collapsible lung airways are believed to give rise to a number of different respiratory noises. Flutter instabilities have been proposed as the origin of respiratory wheezes during forced expiration (e.g. Gavriely *et al.* 1984; 1989), and speech production involves controlled flow-induced vibrations of the vocal chords, which can be modelled as a collapsible tube system (e.g. Berke *et al.* 1991). Similarly bird song involves oscillations of a set of membranes in the avian syrinx. Fee *et al.* (1998) have shown that modulations of bird song display characteristics (such as mode locking and period doubling) of a nonlinear dynamical system, and they provide experimental and theoretical evidence of the primary mechanism being a dynamic flow-structure interaction. Results from a computational

model of this process were presented to the IUTAM Symposium by J. L. van Leeuwen.

Snoring sounds in humans during obstructive sleep apnea have their origins in flow-induced deformation of the soft palate and pharyngeal wall. The Bernoulli effect can induce upper airway collapse and closure (characterised using a simple lumped-parameter model by Gavriely & Jensen 1993, for example), and flow-induced instabilities of the airway wall can then lead to noise production; for a distributed collapsible-tube model of this process see Aittokallio *et al.* (2001). Flow-induced flutter of the soft palate, which can be modelled as a flexible cantilevered elastic plate that can flap as air flows past it (Huang 1995), is an independent source of noise production. In a study presented to the IUTAM Symposium, Balint & Lucey used Navier–Stokes simulations, coupled to plate equations, to show how instabilities of the soft palate can arise either through a flutter mechanism or through so-called static divergence (where the plate undergoes a non-oscillatory sideways displacement); for full details see Balint (2001).

Spontaneous flow-induced oscillations also arise throughout the cardiovascular system. These include cervical venous hum, arising through oscillations of the external jugular vein, which is collapsed because of a low hydrostatic pressure (Danahy & Ronan 1974). Korotkoff sounds heard during sphygmomanometry have been associated with the development of self-excited oscillations of the partially reopened brachial artery (see e.g. Ur & Gordon 1970 and Bertram *et al.* 1989), although alternative mechanisms of noise production have also been proposed, for example by Shimizu & Tanida (1983). Oscillations in coronary blood vessels have also been observed during open-heart surgery (Tsuji *et al.* 1978).

3. Background to theoretical models of collapsible-tube flows

Many of the physiologically observed phenomena described above can be reproduced in laboratory experiments using the 'Starling Resistor,' shown in Fig. 1. Inside a pressure chamber, a thin-walled elastic tube (typically made of latex rubber) is mounted on two rigid tubes. Fluid (typically air or water) is driven through the tube, either by applying a controlled pressure drop $p_{entry} - p_{exit}$ between the ends of the rigid tubes or by controlling the flow rate Q. The external pressure, p_{ext}, can be controlled independently. If p_{ext} exceeds the fluid pressure by a sufficiently large amount, the tube buckles non-axisymmetrically, as sketched in Fig. 1. Flow-structure interactions then lead to a strongly nonlinear relation between pressure-drop and flow-rate, depending on which pressure differences are held fixed as the flow increases (e.g. Conrad 1969). Among these are flow limitation (increasing

$p_{up} - p_{down}$ while keeping $p_{up} - p_{ext}$ fixed limits the maximum possible flux Q) and pressure-drop limitation (increasing Q with $p_{down} - p_{ext}$ fixed limits the maximum possible $p_{up} - p_{down}$). At sufficiently large Reynolds numbers, the system also readily produces self-excited oscillations, and exhibits hysteresis in transitions between dynamical states, multiple modes of oscillations (each having a distinct frequency range) and rich and complex nonlinear dynamics (Bertram 1986; Bertram *et al.* 1990). For full details see Chapter 3.

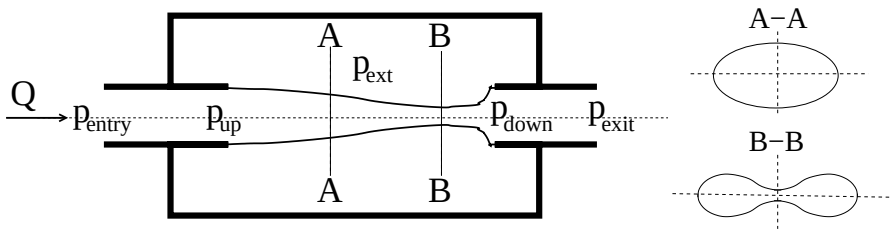

Figure 1. Left: sketch of the typical experimental setup which forms the basis of most theoretical models. Right: tube cross-sections at A–A and B–B.

A closely related physical model system was introduced by Pedley (1992). It consists of a 2D channel, one wall of which has a segment replaced by a membrane under longitudinal tension, as shown in Fig. 2. Viscous flow is driven through the channel by an imposed pressure drop $p_{entry} - p_{exit}$. The external pressure p_{ext} and the internal flow determine the deformation of the membrane. Despite the practical difficulties of producing 2D flows experimentally, this system has attracted considerable theoretical attention since it avoids the complications of fully 3D flows found in the Starling Resistor, while still exhibiting phenomena such as flow limitation and self-excited oscillations.

The earliest theoretical models of flow in collapsible tubes (e.g. Conrad 1969, Katz *et al.* 1969, Bertram & Pedley 1982) were lumped-parameter models in which the system's behaviour is characterised by a small number of scalar variables (such as the cross-sectional area, the transmural pressure and the fluid velocity at the point of strongest collapse, etc.). The temporal variations of these quantities are described by nonlinear ODEs whose numerical solutions can exhibit oscillatory behaviour reminiscent of that observed in experiments. While these models successfully capture many important flow features (such as the crucial role played by the fluid in the rigid parts of the system), they fail to describe such key phenomena as wave propagation. A more sophisticated approach is therefore warranted.

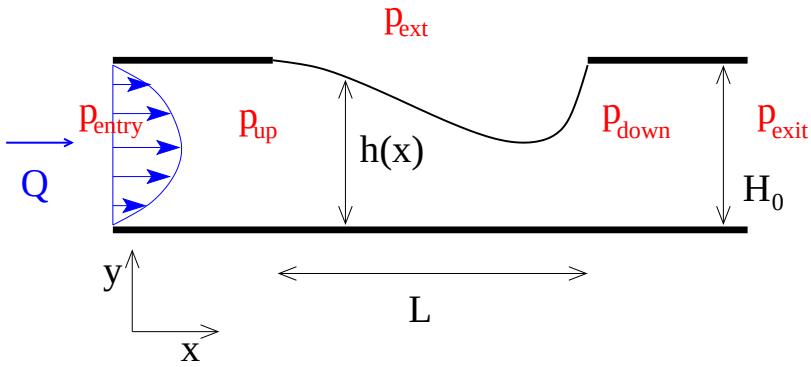

Figure 2. Sketch of the 2D model problem: viscous flow through a channel in which part of one wall has been replaced by an elastic membrane under tension T_0.

4. One-dimensional models

4.1. DERIVATION

Motivated by the successful application of 1D inviscid models for pulse-wave propagation in the arteries, the earliest distributed models of collapsible tube flow were based on a similar mathematical framework. Employing a long-wavelength approximation to the Navier-Stokes equations (including body forces and a 'lumped' representation of small viscous effects), the axial component of the momentum equation is given by

$$\frac{\partial u}{\partial t} + u\,\frac{\partial u}{\partial x} = g - \frac{1}{\rho}\frac{\partial p}{\partial x} - \mathcal{R}u. \tag{1}$$

Here $u = u(x,t)$ is the cross-sectionally averaged axial fluid velocity, $p = p(x,t)$ is the fluid pressure, ρ the fluid density and $\mathcal{R} > 0$ is a friction factor whose value depends on the local cross-sectional area $A(x,t)$ (and also on u in certain circumstances). g represents the gravitational acceleration when the tube is held vertically. The integral continuity equation is

$$\frac{\partial A}{\partial t} + \frac{\partial (uA)}{\partial x} = 0. \tag{2}$$

These equations need to be augmented by a constitutive model for the wall. In the earliest 1D models, this was provided by a functional relationship between the local transmural pressure, $p_{tm}(x,t) = p(x,t) - p_{ext}$, and $A(x,t)$. This relationship is generally referred to as the 'tube law' and has the general form

$$p_{tm}(x,t) = \mathcal{P}(A(x,t),x) \quad \text{or} \quad A(x,t) = \mathcal{A}(p_{tm}(x,t),x), \tag{3}$$

where the vessel's undeformed cross-sectional area, A_0, is characterised by

$$\mathcal{P}(A = A_0) = 0 \quad \text{or} \quad \mathcal{A}(p_{tm} = 0) = A_0. \tag{4}$$

Note that the functional form (3) of the tube law allows for axial variations of the vessel's elastic properties (reflecting, for example, changes in the undeformed cross-sectional area or variations in the vessel's wall thickness and Young's modulus).

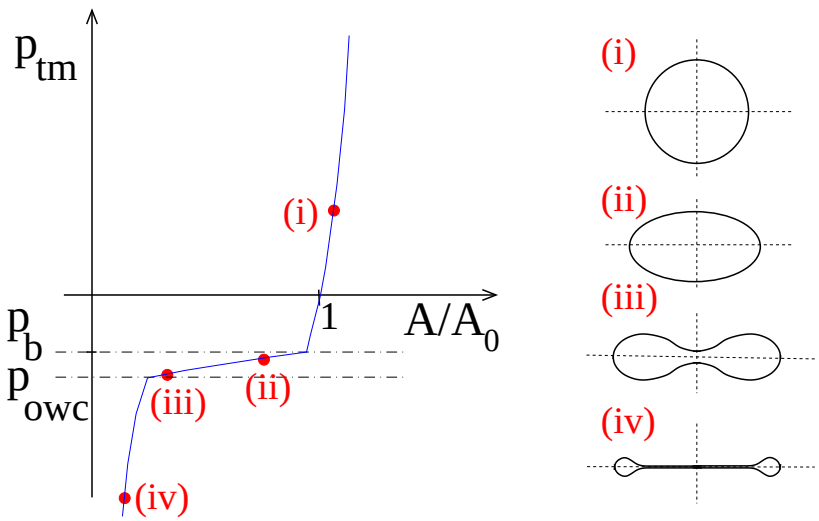

Figure 3. Left: schematic representation of the tube law. Right: typical tube shapes.

The schematic representation of the tube law in Fig. 3 illustrates the drastic change in the wall distensibility (the inverse stiffness)

$$D = \frac{1}{A}\left(\frac{\partial \mathcal{A}}{\partial p}\right) = \frac{1}{A}\left(\frac{\partial \mathcal{P}}{\partial A}\right)^{-1} \tag{5}$$

as the tube's cross-section changes from inflated to collapsed. In the axisymmetrically inflated state, (i) in Fig. 3, any deformation is accompanied by a stretching of the wall. Therefore large changes in transmural pressure are required to induce any change to the vessel's cross-sectional area. The axisymmetric vessel can withstand small compressive loads ($0 > p_{tm} > p_b$). However, when the transmural pressure falls below p_b, the tube buckles non-axisymmetrically, typically to a two-lobed state. Once buckled, only the tube's small bending stiffness resists any further collapse. Hence the vessel

can undergo large changes in cross-sectional area when the transmural pressure changes slightly; see (ii)–(iii) in Fig. 3. As the compression increases further, the vessel's opposite walls come into contact (when $p_{tm} < p_{owc}$) and the wall stiffness increases again as the two outer lobes need to be bent strongly in order to further reduce the cross-sectional area, (iv) in Fig. 3. Various curve fits which approximate the $p_{tm} = \mathcal{P}(A)$ relationship sketched in Fig. 3 and which incorporate the correct solid-mechanical behaviour (see Flaherty *et al.* 1972) have been suggested in the literature; see e.g. Shapiro (1977) or Elad *et al.* (1987).

4.2. STEADY FLOW: CHOKING, FLOW LIMITATION AND ELASTIC JUMPS

Valuable insight into the behaviour of collapsible tubes can be gained from the steady version of equations (1–3). We will initially ignore the effect of gravity ($g = 0$) and assume that the elastic properties of the vessel (and thus the tube law) are independent of axial position. The three steady equations can then be combined to give

$$\frac{1}{A}\frac{dA}{dx} = -\frac{1}{u}\frac{du}{dx} = \frac{-\mathcal{R}u}{c^2 - u^2}, \tag{6}$$

where $uA = Q$ is a constant and

$$c = \sqrt{1/(\rho D)} \tag{7}$$

is the wavespeed of small-amplitude disturbances travelling along the tube (as in pulse-wave propagation). The dependence of the wavespeed c on the tube's stiffness implies that c is much larger in regions where the vessel is inflated than in those where it is collapsed without opposite walls in contact.

Equation (6) predicts an interesting phenomenon, known (in analogy to a related phenomenon in gas dynamics) as 'choking.' Assume that, at the upstream end of the tube, the average fluid velocity u is less than the wavespeed c. Since $\mathcal{R} > 0$, (6) implies that $dA/dx < 0$, i.e. the tube's collapse increases in the direction of the flow. Continuity then requires that $du/dx > 0$, i.e. the flow is accelerated in the streamwise direction. Provided the tube is long enough, we will therefore approach a location at which the 'speed index' $S = u/c \to 1$ and thus $dA/dx \to -\infty$, violating the long-wavelength assumption implicit in the 1D model. Clearly, this situation is physically unrealisable, implying that steady flows are impossible (according to this simple model) if the flow rate becomes so large that u approaches c anywhere along the tube. Alternatively, if $S > 1$ at some point

along the tube, then variations in downstream conditions cannot propagate upstream (since small-amplitude waves travel at speeds $u \pm c$); this underlies the wave-speed mechanism of flow limitation that is believed to operate in the large airways of the lung (Dawson & Elliot 1977; Elliot & Dawson 1977). Several authors speculated that the occurrence of supercritical flow ($u > c$) at some point along the tube might coincide with the onset of self-excited oscillations. Experimental evidence (e.g. Brower & Scholten 1975 and Bonis & Ribreau 1978) appeared first to provide partial support for this view. However Gavriely *et al.* (1989) found that while flow-induced oscillations in a tube with large wall inertia occurred only when the flow was limited, the onset flow speed could be as low as $S \approx 0.3$ (although their definition of wave speed did not take account of wall mass). Later experiments by Bertram & Raymond (1991) and computations by Luo & Pedley (2000) have also cast doubt over a causal link between flow limitation and self-excited oscillations.

Having identified a choking mechanism which is similar to that found in compressible gas flow, one might expect the 1D collapsible tube equations to have shock-like solutions similar to those found in gas flows through Laval nozzles (resembling also hydraulic jumps in shallow-water flows). Experimentally, shock-like structures (known as 'elastic jumps') in collapsible tube flow are easily generated (see e.g. Kececioglu *et al.* 1981). Within the framework of the 1D model, elastic jumps are predicted to occur in situations where supercritical ($S > 1$) flow is generated somewhere in a collapsible tube. Experimentally this is done most effectively by pinching the tube at a far upstream location; the reduction in cross-sectional area increases the fluid velocity u while the associated reduction in wall stiffness simultaneously reduces the wavespeed c. The ensuing supercritical flow is still governed by (6), which now predicts that $dA/dx > 0$. Hence the cross-sectional area A increases and, provided the tube is long enough, the reduction in fluid velocity u now leads to a situation in which $dA/dx \to +\infty$ at some point. As in the case of choking, this locally violates the model's assumptions. However, a shock-like transition region, in which the flow speed is reduced from super- to subcritical, can instead develop upstream of the point where $dA/dx \to +\infty$ would occur. The application of jump conditions (similar to those used in gas dynamics) across the thickness of the elastic jump (Oates 1975, Shapiro 1977, Cowley 1982) establishes how the flow changes as it passes from the supercritical to the subcritical regime. The location of the elastic jump is determined by the downstream boundary conditions, which can influence only the subcritical region of the flow downstream of the jump. Standing waves can appear either upstream or downstream of elastic jumps through the effects of longitudinal bending

or tension, attenuated by viscous effects (McClurken *et al.* 1981; Cowley 1983).

4.3. EFFECTS OF GRAVITY AND NON-UNIFORM TUBE PROPERTIES

As mentioned in Section 2, the venous system is strongly affected by gravitational pressure variations. Inclusion of gravity for a vertical tube changes the steady equation (6) to

$$\frac{1}{A}\frac{dA}{dx} = -\frac{1}{u}\frac{du}{dx} = \frac{g - \mathcal{R}u}{c^2 - u^2}. \tag{8}$$

In the presence of gravity, choking can be avoided because smooth transitions from sub- to supercritical flows are possible if the flow becomes critical ($u = c$) at a location where $g = \mathcal{R}u$. Shapiro (1977) lists a number of other physiologically relevant scenarios in which smooth transitions through $u = c$ are possible. They include **(i)** axial variations of the vessel's elastic properties; **(ii)** spatial variations in the external pressure (representing, e.g., a localised compression as in sphygmomanometry); and **(iii)** variations in the vessel's undeformed cross-sectional area (corresponding to flow in tapered elastic tubes). Properties **(i)** and **(iii)** in particular have been used (for example by Elad *et al.* 1987) to describe flow limitation in the lung: during forced expiration, a sub- to supercritical flow transition arises through non-uniform airway properties, and a super- to subcritical transition can occur further downstream via an elastic jump. Changes in the downstream boundary conditions affect the location of the elastic jump but not the overall flow.

A closely related example is provided by the giraffe jugular vein. Experiments suggest it is in a strongly collapsed state when the giraffe is standing upright, and that the flow in it can be supercritical. Pedley *et al.* (1996) related the position of an elastic jump in the vein to the downstream flow rate Q and the vein's downstream cross-sectional area (which is set at the junction with the distended superior vena cava). Pedley *et al.* (1996) showed that an increase in Q forces the elastic jump to move further downstream, and concluded that, in steady flow, Q cannot exceed the value $Q_{\max}$ for which the elastic jump occurs at the downstream end of the jugular vein.

4.4. UNSTEADY FLOWS AND WAVE PROPAGATION

The full time-dependent equations (1–3) are of hyperbolic character. Kamm & Shapiro (1979) performed a detailed analysis of the linear and nonlinear waves governed by these equations. Particular attention was paid to the time-dependent collapse and refilling of tubes which are subjected to an

instantaneously applied, spatially non-uniform external pressure, a model of compression therapy for deep-vein thrombosis (Kamm 1982, Olson *et al.* 1982, Dai *et al.* 1999).

For a particular choice of the tube law $\mathcal{P}(A)$ and the resistance function $\mathcal{R}$, Cowley (1981) was able to show that equations (1–3) have solutions which have the character of roll-waves in open channel flows (analysed by Dressler 1949). Recently, Brook *et al.* (1999) re-examined the properties of roll-wave solutions in the collapsible-tube equations under less restrictive assumptions. Using a numerical Godunov scheme, they found that roll waves can develop from unstable steady solutions of the 1D collapsible tube equations. Applying time-dependent computations to the problem of blood flow in the giraffe jugular vein described above, Brook & Pedley (2001) showed that for $Q > Q_{\max}$ the flow remains unsteady, but roll waves were not predicted to occur. At the IUTAM Symposium, Brook & Pedley showed that axial variations of the tube properties result in smooth super- to subcritical transitions that are temporally stable. An increase in flow rate is again found to move the position of the critical point (at which u smoothly falls below c) further downstream. Thus a maximum flow rate is predicted above which the critical point would no longer be located inside the collapsible tube; for flow rates in excess of this value, the flow must therefore be unsteady; see Brook (1997) and Brook & Pedley (2001).

At the IUTAM Symposium, Berkouk, Capenter & Lucey presented a study of the propagation of pressure waves along the fluid-filled spinal cord (Carpenter *et al.* 1999, 2001*a*, 2001*b*). The model consists of two co-axial tubes: the rigid outer tube was taken to represent the bony part of the spine (the subarachnoid space), while the elastic inner tube represents the spinal cord containing cerebrospinal fluid. It was shown that the propagation of pressure waves in the cerebrospinal fluid is strongly affected by the presence of blockages in the outer tube, a situation that is characteristic of syringomyelia, a disease of the spinal cord.

4.5. FLUTTER AND STATIC-DIVERGENCE INSTABILITIES

The models described so far are relevant for systems in which the inertia of the fluid dominates that of the wall. In experiments mimicking flows in lung airways, however, in which air is blown through thin-walled tubes, wall inertia cannot be neglected. Drawing on studies in aeroelasticity, a number of workers have presented investigations of the stability of potential flows in channels where one or both walls of the channel are some form of heavy spring-backed plate with bending stiffness and subject to longitudinal tension. In these studies it was assumed that the flow domain is unbounded in the streamwise direction, and a linearised (small-amplitude)

analysis was used to obtain dispersion relations for waves of a given wavelength, assuming also that the mean velocity profile is uniform across the channel. Grotberg & Davis (1980), for example, showed how such a system, in the absence of any dissipation, exhibits an oscillatory flutter instability, for which a downstream-propagating wave can grow temporally. The introduction of a small amount of wall damping had the dramatic effect of changing the instability to one of static divergence (a non-oscillatory instability in which hydrodynamic pressures overcome the restoring forces in the channel wall), as was also found by Weaver & Païdoussis (1977) and Matsuzaki & Fung (1977). (Choking, described in Section 4.2, can also be regarded as a manifestation of static divergence.) Only by adding dissipation to the fluid (using a Darcy-type term that was later justified by Grotberg & Shee 1985), making pressure and displacement act out of phase with one another so that the fluid could do work on the wall, could an oscillatory travelling-wave flutter (TWF) instability be recovered (Grotberg & Reiss 1984). In this sense TWF is a Class B instability (in the energy classification of Benjamin 1963 & Landahl 1962), in that it is destabilised when energy is transferred from the flow to the wall. Even though these investigations involved 2D potential flows, Walsh (1995) has demonstrated that their long-wave (1D) limit captures the dominant physical behaviour, while showing also that coupling between axial and transverse motion for curved shells (such as the trachea) can be dynamically significant (see also Walsh *et al.* 1991).

These models capture two fundamental mechanisms of instability in infinitely long fluid-filled channels (static divergence and TWF), and demonstrate the important role of dissipation in both the fluid and the wall, and of the mechanical model chosen for the wall. However to understand the role of such instabilities in the Starling-Resistor, in which the flexible segment has finite length, alternative models and solution techniques are required.

4.6. 1D MODELS OF FLOW IN THE STARLING RESISTOR

4.6.1. *Model development*

To describe flows in the Starling Resistor (Fig. 1), the governing equations (1–3) must be supplemented by boundary conditions describing the rigid parts of the system, which are known both experimentally and from lumped-parameter models to have a major effect on both steady and unsteady flows. Typical pressure-flux relationships that incorporate the effects of viscous resistance (R) and fluid inertia (I) in the upstream and down-

stream segments are of the form

$$\begin{aligned} p_{entry} - p_{up} &= R_{up}Q_{up} + I_{up}\frac{dQ_{up}}{dt}, \\ p_{down} - p_{exit} &= R_{down}Q_{down} + I_{down}\frac{dQ_{down}}{dt}. \end{aligned} \tag{9}$$

The tube area must also be prescribed at either end of the collapsible segment, where it is mounted onto the rigid pipes (e.g. $A_{up} = A_{down} = A_0$, where A_0 is defined in (4)). However an immediate problem with the model given by (1–3) is that it is only possible to prescribe the cross-sectional area at a single (say, upstream) location. To overcome this problem, McClurken *et al.* (1981) augmented the tube law (which only represents the effect of the tube's transverse bending stiffness) by terms which represent the effects of the axial wall elasticity. Given that in a strongly collapsed state the aspect ratio of the tube's cross-section is large, McClurken *et al.* (1981) suggested that the flow in such a tube would be similar to the flow between two parallel membranes. Provided the tube is subject to a large axial tension T_0 (as are many biological vessels), and that wall inertia can be neglected, the constitutive equation for the wall can be written as

$$p_{tm} = \mathcal{P}(A) - T_0\,\frac{\partial^2 A}{\partial x^2}. \tag{10}$$

Mathematically, the inclusion of the axial-tension term increases the order of the governing equation and thus allows the application of additional boundary conditions. Furthermore, it makes the system dispersive, allowing sufficiently short waves to propagate upstream against any oncoming flow. Representation of tension in this way was one reason the simpler 2D channel flow illustrated in Fig. 2 attracted subsequent interest, and indeed if $\mathcal{P}(A)$ is removed from (10), and A in (2) and (10) is replaced by the width $h(x,t)$, the resulting equations then apply directly to this simpler system, provided membrane slopes are sufficiently small.

A further significant improvement to the 1D model was proposed and analysed by Cancelli & Pedley (1985). In earlier lumped-parameter models (e.g. Bertram & Pedley 1982), it had been found that the energy loss in the separated-flow region downstream of the point of strongest collapse played an important role in the development of self-excited oscillations. In particular, if this energy loss was completely neglected (corresponding to attached, inviscid flow with complete pressure recovery, as in Fig. 4a), the tube was found always to choke if the flux was increased sufficiently (i.e. $A \to 0$ at some point along the length of the collapsible tube in finite time via a static divergence instability). Cancelli & Pedley (1985) showed that

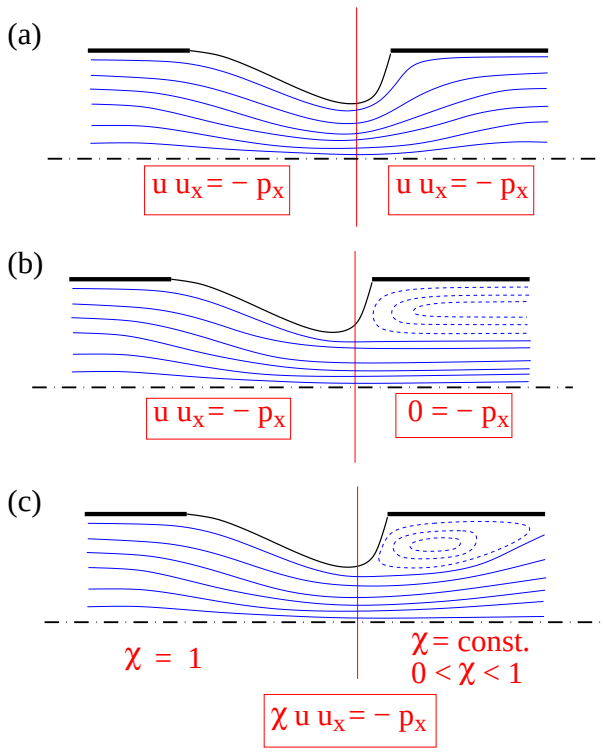

Figure 4. Models of flow separation in a collapsible tube: (a) Attached flow; no pressure loss. (b) Ideal separation; parallel-sided jet downstream of the separation point; no pressure recovery. (c) An intermediate case: $0 < \chi < 1$ downstream of the separation point corresponds to partial pressure recovery.

such behaviour persisted in a 1D inviscid model even when the dispersive effects of longitudinal tension were accounted for. In contrast, if the energy loss associated with flow separation was made as large as possible (corresponding to the formation of a parallel-sided jet beyond the narrowest point in the tube, along which there is no pressure recovery, as in Fig. 4b), Bertram & Pedley (1982) found that steady flow was always possible and no oscillations were predicted. They found that self-excited oscillations arose only if some pressure recovery was allowed. To represent this effect in a 1D framework, Cancelli & Pedley (1985) replaced the inviscid momentum equation (1) by

$$\frac{\partial u}{\partial t} + \chi\, u\, \frac{\partial u}{\partial x} = -\frac{1}{\rho}\frac{\partial p}{\partial x}, \tag{11a}$$

where

$$\left.\begin{array}{ll}\chi = 1 & \text{upstream} \\ 0 < \chi < 1 & \text{downstream}\end{array}\right\} \text{ of the separation point.} \tag{11b}$$

(The small viscous losses represented by $\mathcal{R}$ in (1) were found to be of minor importance and were therefore neglected.) Fig. 4 illustrates the idea behind this approach and shows that (11a,b) are intermediate between the extreme cases of no separation ($\chi \equiv 1$) and perfect separation ($\chi = 0$ downstream of the separation point). Estimates for χ were based on the steady Borda–Carnot condition. Cancelli & Pedley's (1985) theory also allowed for the motion of the separation and attachment points by linking their position to the value of the pressure gradient (although the only way for the dissipative term $(1-\chi)uu_x$ to vary smoothly across the separation point is to choose this point to coincide with that at which $u_x = 0$). Significantly, they found that fixing the location of the separation point was sufficient to suppress oscillations.

4.6.2. *Computational results*

Cancelli & Pedley's (1985) numerical solution of the new time-dependent equations showed that, as in the lumped parameter model, self-excited oscillations occurred only if $0 < \chi < 1$ downstream of the assumed point of flow separation. Following Cancelli & Pedley's (1985) initial computations, Reyn (1987) and Jensen & Pedley (1989) used phase-plane techniques to investigate systematically the existence and non-existence of steady solutions of this model, and demonstrated the existence of multiple steady states. An important effect of dissipation due to flow separation was to reduce the tendency of the tube to choke, and to increase the range of parameters over which a steady solution could exist. Typical steady flow states are illustrated in Fig. 5. Jensen (1990) then analysed the stability of the steady solutions and identified distinct modes of oscillation, each with its own range of frequencies, capturing a key qualitative feature of experiments (Bertram *et al.* 1990, 1991). A weakly nonlinear analysis was employed to explore interactions between these different modes.

In addition, many authors (e.g. Matsuzaki & Matsumoto 1989, Jensen 1992, Matsuzaki *et al.* 1994, Hayashi *et al.* 1998, Ikeda & Matsuzaki 1999) performed detailed numerical simulations to explore the time-dependent behaviour of this and closely related models. Matsuzaki and co-workers refined the representation of energy losses in the region of separated flow; Hayashi and co-workers replaced the dissipative term with a distributed frictional term similar to that in (1). All these numerical studies exhibited self-excited oscillations of considerable complexity. While care is required

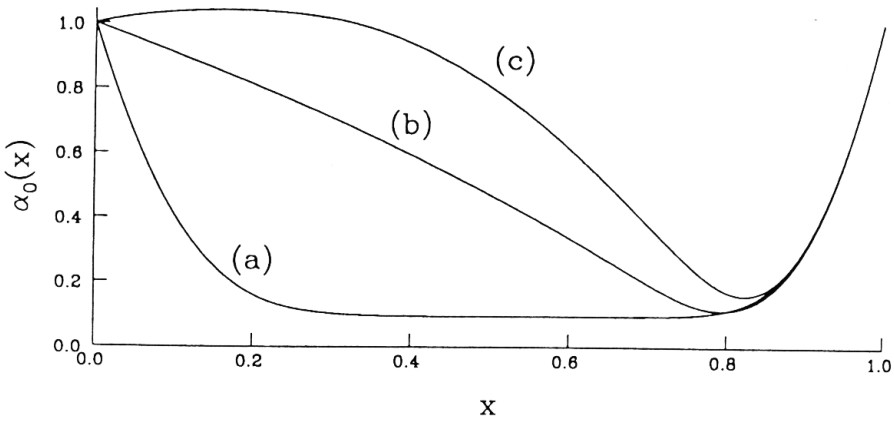

Figure 5. Wall shapes predicted by Cancelli & Pedley's 1D model: an increase in flow rate ($a \to b \to c$) at constant downstream transmural pressure reopens the tube. The flow is assumed to separate beyond the constriction. From Jensen (1992).

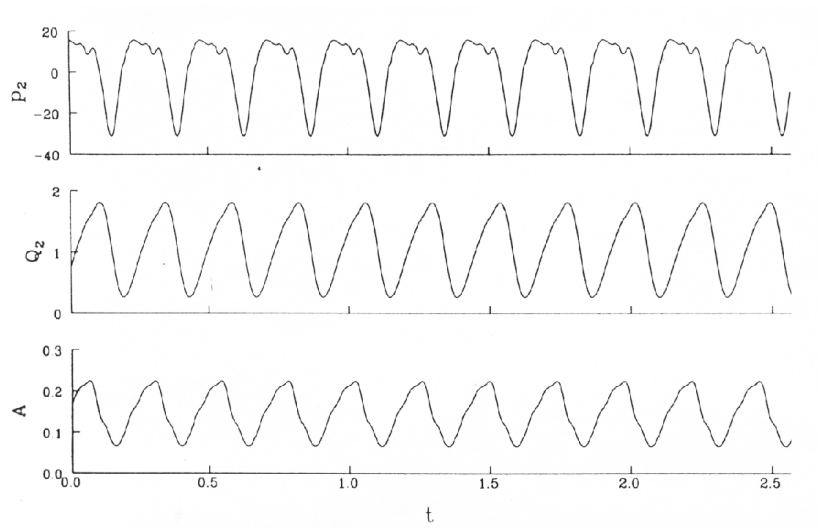

Figure 6. Time-traces of the downstream pressure, flow rate and the minimum cross-sectional area during a self-excited oscillation. From Jensen (1992).

in solving this problem numerically (to avoid generating spurious numerical oscillations), there is convincing evidence that these studies captured genuine oscillatory behaviour, and there is even evidence of chaotic dynamics

(Jensen 1992). Nonlinear periodic oscillations obtained from computations are illustrated in Fig. 6.

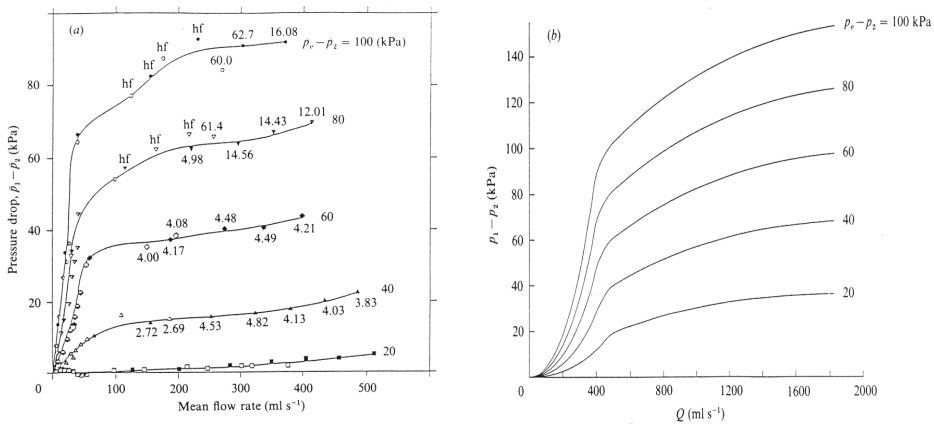

Figure 7. Pressure drop through the tube vs. flow rate for fixed downstream transmural pressure. (a) Experimental results of Bertram (1986) (numbers adjacent to symbols denote frequency of oscillations; for these cases time-averaged pressures are recorded); (b) numerical predictions from the 1D model of Jensen & Pedley (1989).

Despite the use of *ad hoc* assumptions, 1D models can reproduce steady behaviour with reasonable quantitative accuracy. Fig. 7, for example, shows how such a model predicts pressure-drop limitation, and the corresponding experimental results. Major qualitative features of unsteady flows, such as multiple modes of oscillation, can also be simulated with qualitative success. The key ingredients for the prediction of low-frequency oscillations in both lumped and 1D models therefore appear to be **(i)** representation of fluid inertia (introduction of wall inertia can introduce additional higher frequency modes); **(ii)** representation of dissipation in the system, either distributed along the collapsible tube or confined to the separated flow region (either of which can introduce a phase difference between pressure fluctuations and wall displacement, overcoming the tendency of the tube to collapse directly via static divergence); and **(iii)** strong coupling of the flow in the collapsible tube to the rigid upstream and downstream segments via (9).

4.6.3. *Links with flutter instabilities*

The connection between oscillations in the Starling resistor and travelling-wave-flutter identified in potential-flow calculations is not directly obvious,

because of the neglect of wall inertia in many of the computational studies and the profound influence of the rigid parts of the system. However some insight into their relationship can be obtained by examining the situation in which the longitudinal tension T_0 in (10) is large, specifically

$$\mathcal{T} \equiv \frac{T_0 A_0}{\rho U_0^2 L_0^2} \gg 1, \quad \text{where} \quad U_0 \equiv \frac{p_{entry} - p_{exit}}{\rho \mathcal{R} L_0 + (R_{up} + R_{down}) A_0} \tag{12}$$

is the speed of the mean flow through the system assuming $A = A_0$ along the length L_0 of the collapsible segment (the total pressure drop balancing the viscous resistances defined in (1) and (9)). The large tension ensures that the tube remains almost uniform ($A \approx A_0$ in $0 \le x \le L_0$), that its shape is insensitive to the magnitude of the external pressure (unless of course $|p_{ext}|$ is very large) and that transverse elastic stresses (represented by $\mathcal{P}(A)$ in (10)) are not significant. Rather like a stretched string, the Starling Resistor then admits a family of discrete, high-frequency normal modes in which the tube wall oscillates in and out (with one or more half-wavelengths along its length) and the fluid inside the tube oscillates backwards and forwards. To illustrate, we write $A = A_0 + \mathrm{Re}(\hat{A}(X)E)$, $u = \mathrm{Re}(\hat{u}(X)E)$, where $x = L_0 X$, $E \equiv \exp(i\beta(A_0 T_0/\rho L_0^4)^{1/2} t)$ and β is a dimensionless frequency, and then linearise (1, 2, 9, 10) about the uniform state; the dominant terms at high frequencies are unsteady fluid inertia in both the compliant and rigid parts of the system and membrane tension (neglecting gravity in (1) and $\mathcal{P}(A)$ in (10)). The perturbation velocity along the collapsible segment then turns out to satisfy

$$\hat{u}'''' - \beta^2 \hat{u} = 0 \qquad (0 \le X \le 1), \tag{13a}$$

$$\hat{u}'(0) = 0, \qquad \hat{u}'''(0) - \beta^2 (A_0 I_{up}/\rho L_0)\hat{u}(0) = 0, \tag{13b}$$

$$\hat{u}'(1) = 0, \qquad \hat{u}'''(1) + \beta^2 (A_0 I_{down}/\rho L_0)\hat{u}(1) = 0, \tag{13c}$$

with area fluctuations given by $\hat{A}(X) = -A_0 \hat{u}'(X)/i\beta L_0$. This fourth-order problem can be solved to obtain a family of eigenmodes with discrete frequencies $0 < \beta_1 < \beta_2 < \ldots$. Taking the first mode plus a mean flow as the leading-order term in an expansion in powers of $\mathcal{T}^{-1/2}$, one obtains at the following order the linear system (13) with forcing terms arising from advective inertia and viscous dissipation. Applying a solvability condition leads to a condition on the growth rate of the normal modes: the growth rate is positive when

$$\hat{u}^2(0) - \hat{u}^2(1) > \frac{R_{up} A_0}{\rho U_0} \hat{u}^2(0) + \frac{R_{down} A_0}{\rho U_0} \hat{u}^2(1) + \frac{\mathcal{R} L_0}{U_0} \int_0^1 \hat{u}^2 \, \mathrm{d}X. \tag{14}$$

Provided $\hat{u}^2(0) > \hat{u}^2(1)$ (which computations indicate is the case for $I_{down} > I_{up}$, since large downstream inertia suppresses velocity fluctuations at $X = 1$), as the pressure drop across the system increases, U_0 increases through the threshold defined by (14) and normal mode oscillations can become unstable, extracting more energy from the mean flow than is lost to viscous dissipation throughout the system. These oscillations can therefore be regarded as a form of flutter, although in this spatially bounded system they are distinct from convectively unstable travelling waves that arise also in either potential-flow models (e.g. Grotberg & Reiss 1984) or in studies of thin falling liquid films, which are governed by a closely related set of PDEs (Chang & Demekhin 1996).

The analysis leading to (14) was presented to the IUTAM Symposium by Jensen (2001) (for a very similar set of governing equations), who showed also that (14) agrees well with both a stability analysis for arbitrary T_0 and numerical solutions of the full equations. At lower tensions, Jensen's (2001) 1D model also exhibits multiple nonlinear static solutions (arising via static divergence instability), and remarkably intricate oscillations exhibiting, for example, a well-defined period-doubling cascade towards chaos. However, while the stability threshold (14) is effective in understanding 1D model systems in the high-tension limit, it is physically inconsistent: at high frequencies, dissipation is likely to be confined to thin viscous boundary layers that are very poorly described by quasi-steady dissipative terms as simple as that in (1). This reflects the deficiencies present in any 1D model of a high-Reynolds-number flow, and motivates the analysis of more rational 2D systems.

5. Two-dimensional models

5.1. THE MODEL PROBLEM

Given the large resources required for the numerical solution of the 3D problem, much recent activity has focussed on the 2D deformable channel problem illustrated in Fig. 2. The flow is governed by the 2D Navier–Stokes equations

$$\rho\left(\frac{\partial u_i}{\partial t} + u_j\frac{\partial u_i}{\partial x_j}\right) = -\frac{\partial p}{\partial x_i} + \mu\frac{\partial^2 u_i}{\partial x_j^2} \quad \text{and} \quad \frac{\partial u_j}{\partial x_j} = 0, \tag{15}$$

where μ is the fluid's viscosity and $\mathbf{u}(\mathbf{x}, t)$ the 2D velocity field. No-slip and kinematic conditions are imposed at the walls and a prescribed parabolic velocity profile may be imposed at the inlet. The wall is typically modelled as a membrane under axial tension T_0, whose deformation (characterised

by the variable channel width $h(x)$) is assumed to be governed by

$$p - p_{ext} = T_0\ \kappa, \tag{16}$$

where κ is the wall curvature, which can be approximated by $\kappa \approx -d^2h/dx^2$ if the membrane slope is small, as in (10). The flow can then be parameterised by a Reynolds number $Re = \rho U_0 H_0/\mu$ based on the inlet channel width H_0 and an inlet flow speed U_0, and a dimensionless tension parameter $T = T_0/H_0\rho U_0^2$.

Pedley (1992) studied this problem in the lubrication-theory limit (assuming small membrane slope and low Re), and showed how steady solutions may break down if the fluid shear stress reduces the wall tension to zero at some point along the wall. Matsuzaki & Fujimura (1995) showed later that inclusion of bending stiffness in (16) ensures the existence of steady solutions for all values of the tension. Jensen (1998) also used lubrication theory to obtain explicit pressure-flow relations for a highly collapsed channel that exhibits flow and pressure-drop limitation through purely viscous mechanisms.

The remaining studies of this problem have employed either direct numerical methods or high-Reynolds-number asymptotics. In numerical studies (details of which are given below), a moving mesh was employed to discretise the 'Arbitrary Lagrangian Eulerian' form of the Navier-Stokes equations by finite elements. The fluid-mesh update in response to the movement of the wall was typically performed by variants of Kistler & Scriven's (1983) 'Method of Spines'. Two different methodologies were employed to obtain coupled solutions of the fluid and solid equations. In the segregated approaches of Lowe & Pedley (1995), Luo & Pedley (1995) and Liang *et al.* (1997), the fluid and solid equations were discretised independently and a coupled solution was obtained by a fixed-point iteration between the two domains. All subsequent work was based on a fully-coupled approach in which a global Newton–Raphson method was employed to solve the large system of nonlinear algebraic equations which arises from a coupled discretisation of both sets of equations. The fully-coupled approach is more difficult to implement but tends to provide a much more robust procedure. In fact, most authors found the use of a fully-coupled approach to be necessary to obtain converged solutions for the simulation of time-dependent problems with significant fluid-structure interaction.

5.2. STEADY FLOW

5.2.1. *Numerical studies*

Following Lowe & Pedley's (1995) initial study of zero-Reynolds-number flow in collapsible channels, Rast (1994) and Luo & Pedley (1995) per-

formed detailed studies of the system's behaviour at finite Reynolds number. Fig. 8 illustrates some of Rast's (1994) results and shows the streamlines for the flow through a strongly collapsed channel. Downstream of the point of strongest collapse the flow field is similar to that found in the flow over a backward facing step (Armaly *et al.* 1983). As Re increases, a sequence of recirculating eddies develops on alternate sides of the channel. Note that the flow field immediately downstream of the separation point is not dissimilar to that assumed in Cancelli & Pedley's (1985) 1D representation of flow separation.

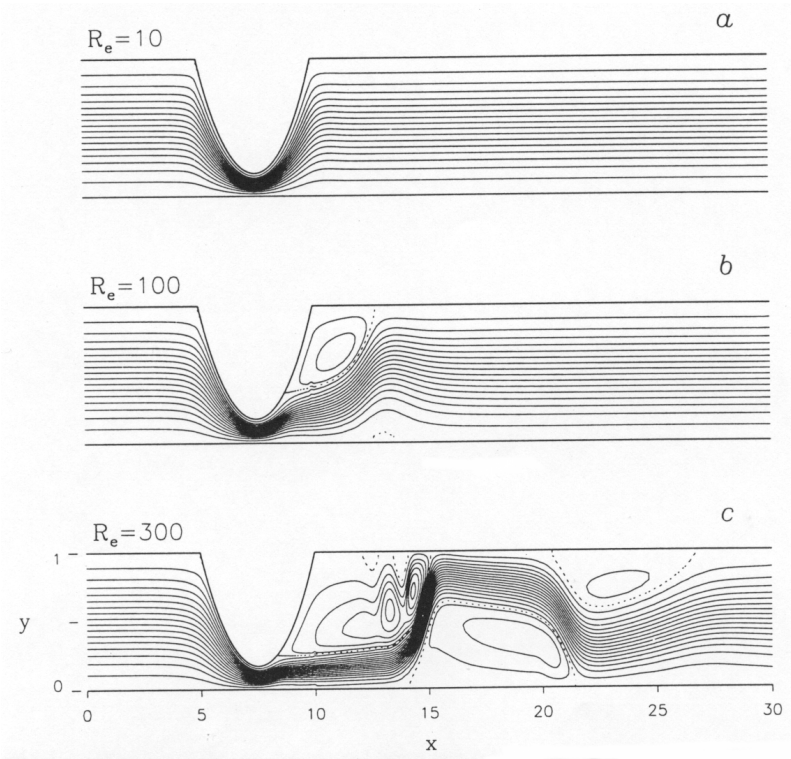

Figure 8. Streamlines for steady finite Reynolds number flow through a collapsible channel; from Rast (1994).

When studying the system's response to changes in the wall tension T, Luo & Pedley (1995) noticed that it became increasingly difficult to obtain converged solutions as the tension was reduced. No solutions could be obtained if the tension was decreased below some critical value T_c, which was dependent on Re. It was observed that T_c was close to the tension

T_b at which the wall began to bulge out near the upstream end of the elastic segment (resulting in a wall shape similar to that shown in Fig. 9a below). Bulging of the wall presents computational difficulties, since the fluid pressure and the vorticity develop singularities at the convex upstream corner. In the context of the collapsible-channel problem, these singularities were first analysed by Lowe & Pedley (1995). The development of sharp corners (and the associated singularities in the flow field) can be suppressed by including bending stiffness into the wall model. This was first done by Liang *et al.* (1997), whose linear Eulerian wall model represented the elastic section as a pre-stressed elastic beam. At the IUTAM Symposium, Cai & Luo (2001) presented a model which incorporated bending and extensional stiffness into a geometrically nonlinear Lagrangian representation of the wall; they also analysed how bending stiffness affects the structure of the flow near the ends of the flexible segment.

5.2.2. *Asymptotic models*

Only a few studies are available in which high-Reynolds-number asymptotic analysis has been applied to steady flows in deformable tubes and channels. Tutty (1984) solved the boundary-layer equations coupled to a tube law to integrate into a singular choke point over a long $O(Re)$ lengthscale (recovering the basic choking phenomenon described in Section 4.2), while Rothmayer (1989) used interactive triple-deck theory to describe so-called 'free interaction' solutions over shorter lengthscales for nearly uniform symmetric channels. This work builds on the framework of Smith (1976*a*,*b*), who showed how to couple viscous boundary layers on either wall of a long channel to an inviscid rotational core flow between them. More recent work in this direction by Guneratne (1999) and Guneratne & Pedley (2001) was reported to the IUTAM Symposium by Pedley. At high T or small transmural pressure, the membrane deflection is weak enough that the wall displacements are of comparable magnitude to the boundary-layer thickness. Displacement of the wall, induced either by the external pressure p_{ext} or by flow-induced pressure variations, causes a sideways displacement of the inviscid core flow. Guneratne solved the interactive boundary-layer equations to determine steady flow configurations, formally assuming that the channel length $L_0 = H_0\lambda$ is large ($Re^{1/7} \ll \lambda \ll Re$) and the boundary layers are narrow (having thickness of order $H_0(\lambda/Re)^{1/3}$). The special case $\lambda = O(Re^{1/7})$ captures the effect of a cross-stream pressure gradient, although this turns out not to be particularly significant to the overall solution structure. With $p_{ext} = 0$, the uniform state loses stability to eigensolutions in which the membrane is either weakly indented or dilated, or both. Stability is lost through a sequence of transcritical bifurcations, with mem-

brane tension a bifurcation parameter. Imposition of nonzero p_{ext} acts as a symmetry-breaking effect. When the upstream transmural pressure is held constant the system exhibits abrupt jumps between solutions and there are even ranges of T for which no steady solution could be found. Guneratne demonstrated that the system exhibits a rich variety of nonuniform steady states, reminiscent of those identified in the inviscid 1D models of Jensen & Pedley (1989) and Reyn (1987), and which presumably are once again a nonlinear manifestation of static divergence instability. Although the stability of these solutions to unsteady disturbances was not determined, their richness points to even greater complexity in the full dynamic problem.

5.3. UNSTEADY FLOW AND SELF-EXCITED OSCILLATION

5.3.1. *Fundamental modes of instability*

Before discussing computational studies of unsteady 2D flows, it is helpful to digress briefly to mention studies of the linear stability of 2D flows in unbounded channels having deformable walls. For more detailed reviews of much of this work see Davies & Carpenter (1997*a*) and Chapter 4 of this volume. These studies, extending the simpler potential-flow models described in Section 4.5, identify three primary modes of instability for channels with spring-backed walls having bending stiffness, longitudinal tension, damping and inertia. As we have seen already, travelling-wave flutter (TWF) is a convective, oscillatory Class B instability (in the Benjamin-Landahl energy classification), destabilised when energy is transferred from the flow to the wall. These waves are stabilised by wall damping. In their long-wave analysis of the Orr-Sommerfeld problem for disturbances to Poiseuille flow in a compliant channel, Davies & Carpenter (1997*a*) show how TWF is destabilised by effects confined to critical layers (which put pressure and wall displacement out of phase, allowing the flow to do work on the wall, an effect described also by Huang 1998), but is stabilised by viscous effects in wall (Stokes) layers. Tollmien–Schlichting (TS) waves are intrinsic hydrodynamic modes of instability that are present even when the channel walls are rigid; these are Class A waves (stabilised when energy is transferred from the flow to the wall, and destabilised by wall damping).

Finally, static divergence is a direct, non-oscillatory (or very low frequency) instability that is Class A or C (C being one that is insensitive to energy transfer between the flow and the wall). In addition to these three primary modes, further modes can arise through mode coalescence, so that TWF and TS modes can combine to give rise to a powerful Class C flutter instability. Larose & Grotberg (1997) also identified an apparently distinct long-wave instability of developing flow in a compliant channel, and Davies & Carpenter (1997*b*) showed how energy can be transferred from TS waves

to flow-induced surface instabilities at junctions in flows over compliant panels of finite length. Huang (2001) has also examined the linear stability of the configuration shown in Fig. 2 when the membrane is nearly flat, and shown how both flutter and divergence modes can arise when the membrane has significant inertia. It should be borne in mind that **(i)** the strongly nonlinear phenomena to be described below presumably have their origins in these fundamental instabilities and **(ii)** neglecting effects such as bending stiffness or wall damping may be dangerous because these can be singular limits of the full stability problem.

5.3.2. *Computational studies*

Unsteady finite-Reynolds-number flows in collapsible channels have been computed by Luo & Pedley (1996, 1998, 2000), Liang *et al.* (1997) and Pedrizzetti (1998). For time-dependent problems, the application of the no-slip condition on the channel wall poses a subtle problem because the Eulerian wall model (16) determines the wall's overall shape but not the position of individual material particles. Therefore certain *ad hoc* assumptions regarding the wall displacement field have to be made when matching the fluid and wall velocities. Luo & Pedley (1996) considered two reasonable assumptions (wall displacements either in the vertical direction or in the direction normal to the wall's instantaneous shape) and showed that the results obtained with the two boundary conditions differed only slightly. Cai & Luo's (2001) new Lagrangian wall model will avoid this ambiguity in future time-dependent simulations. Given the important role that the wall tension T appeared to play for steady flows, Luo & Pedley (1996) investigated the system's time-dependent behaviour for different values of T. They found that, for sufficiently large Reynolds number, self-excited oscillations developed when the tension was reduced below a critical value, T_u. They reported that T_u tended to be close to but not identical to the value T_b at which the upstream end of the collapsible segment began to bulge out, although without varying many of the remaining parameters in the problem the significance of bulging is hard to estimate. For values of T just below T_u, the wall performed sustained harmonic oscillations. As the tension was reduced further, the system appeared to undergo several period-doubling bifurcations and carried out increasingly complex oscillations, many features of which were reminiscent of those observed in the experiments of Bertram *et al.* (1990).

5.3.3. *Vorticity waves*

Fig. 9 shows the wall shapes and instantaneous streamlines in a channel which is undergoing such large-amplitude self-excited oscillations. One of

the key features in the flow field is the generation of travelling waves downstream of the oscillating wall. The waves are very similar to the 'vorticity waves' which are generated in 2D channels in which an elastic segment of one wall is oscillated in a prescribed manner (Stephanoff *et al.* 1983; Pedley & Stephanoff 1985; Ralph & Pedley 1988, 1989, 1990). Comparison in these studies between experiment and a weakly nonlinear theoretical analysis supports the view that small-amplitude vorticity waves are sustained through an inviscid mechanism, involving perturbations of the vorticity in the oncoming Poiseuille flow, and that they have a wavelength $O(St^{-1/3})$ that is approximately independent of Re, where $St = (H_0^2\omega/\mu) \ll 1$ is the Strouhal number of the oscillation (ω being the oscillatory frequency). In a similar way, flow forced by unsteady pressure gradients through channels with fixed asymmetric indentations also generates vorticity waves (Sobey 1985; Tutty 1992; Tutty & Pedley 1993; Rosenfeld 1995), provided the forcing frequency is in an appropriate range.

The origin of vorticity waves is of fundamental interest to the present problem. The analysis of Bogdanova & Rhyzov (1983) of TS waves in plane Poiseuille flow, using the interactive boundary-layer framework developed by Smith (1976*a*,*b*), shows that downstream-propagating TS waves with wavelength $aRe^{1/7}$ can grow spatially if $StRe^{3/7}$ exceeds a critical value; Smith & Burggraf (1985) went on to suggest a link between large amplitude lower-branch TS waves and vorticity waves. These observations are consistent with the computations of Rosenfeld (1995) who shows how, as St increases with Re fixed for oscillatory flow through a channel with one indented wall, waves (presumably vorticity waves) are generated when St is of magnitude comparable to $Re^{-3/7}$. The waves change character as St increases, suggesting alternative mechanisms are operating, and are suppressed as St rises above unity.

These observations raise some immediate questions. Are the self-excited oscillations computed by Luo & Pedley (1996) generated by a primary flutter mechanism, which then forces secondary vorticity (TS) waves, or do vorticity waves generate the primary instability? Might a combined TS/TWF mode (such as reported by Davies & Carpenter 1997*a*) be driving the oscillations? And if any one of these mechanisms operates, how universal is it as membrane properties and upstream and downstream flow conditions are varied?

While we are far from a satisfactory answer to these questions, some useful evidence is provided by results of a recent combined asymptotic and computational study (Jensen & Heil 2002) suggesting that the high-tension flutter instability described in a 1D model by Jensen (2001) (see Section 4.6.3) has a direct analogue in two dimensions. A formal asymptotic

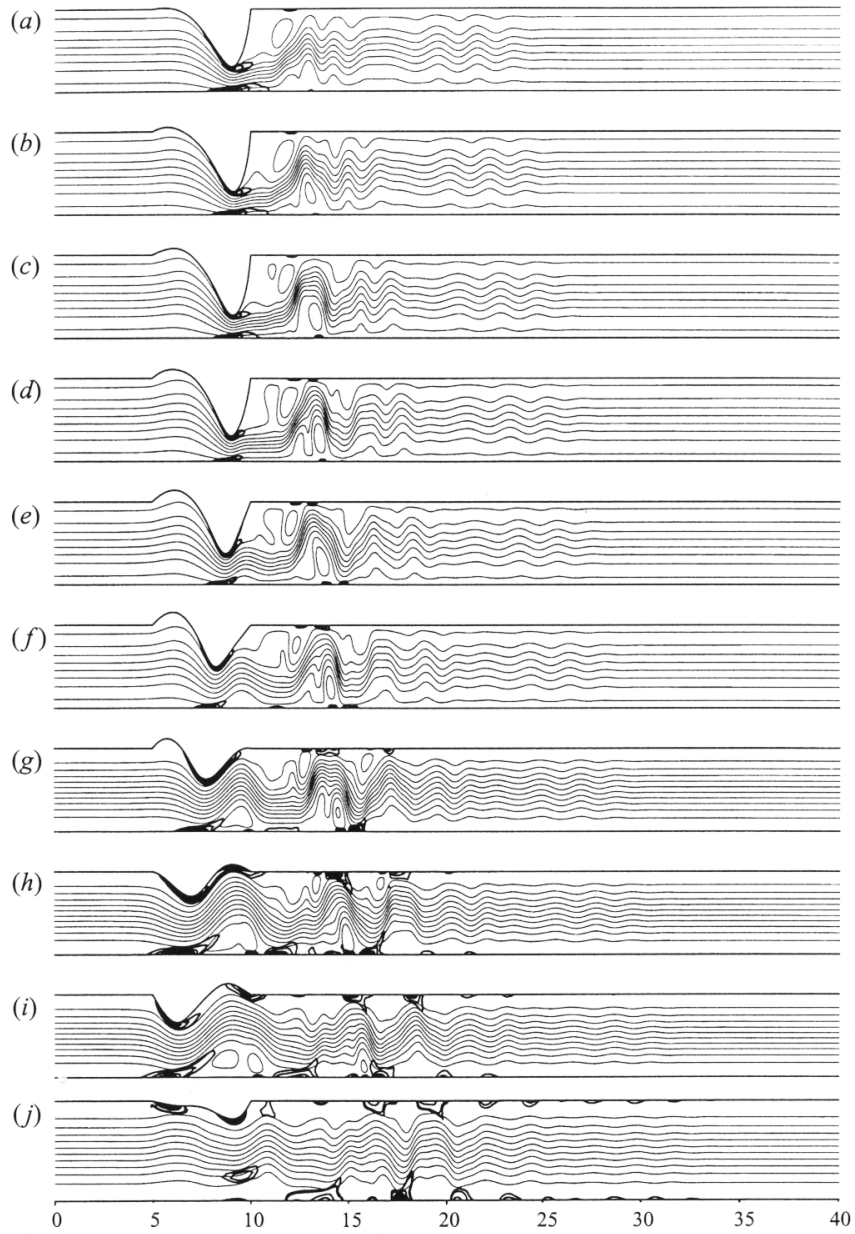

Figure 9. Wall shapes and instantaneous streamlines during self-excited oscillations of a collapsible channel; from Luo & Pedley (2000).

approximation of the 2D problem illustrated in Fig. 2, assuming $Re \gg 1$, $T \gg 1$ and membrane length $L_0 \gg H_0$, predicts that under suitable conditions the normal modes of the system described by (13) can become unstable and grow into self-excited oscillations when the Re exceeds a threshold Re_c of the form

$$Re_c \propto T^{1/2}\beta \left[\frac{\int_0^1 \hat{A}_X^2 \, \mathrm{d}X}{\hat{A}_X^2(1) - \hat{A}_X^2(0)} \right]^2 . \tag{17}$$

Here β and $\hat{A}(X)$ are exactly the eigenfrequency and area perturbation computed using the 1D model via (13) (with I_{up} and I_{down} defined appropriately). Again, the analysis indicates that a necessary condition for this instability to occur is that $I_{down} > I_{up}$. Since dissipation is confined to unsteady Stokes layers at high frequencies, Re_c scales with $T^{1/2}$, an important feature that was not captured in the analogous 1D result (14). It is also striking that dissipation in the rigid parts of the system does not contribute to the stability boundary in this limit. Predictions such as (17) show good agreement with Navier–Stokes computations (for details see Jensen & Heil 2002), supporting the view that flutter alone can provide the primary mechanism of instability, at least when membrane tension is large.

5.3.4. *Dissipation and flow limitation*

Luo & Pedley (1996) computed the rate of dissipation in the fluid in order to check Cancelli & Pedley's (1985) assumption that most of the energy loss, which had been found to be crucial for the development of self-excited oscillations, occurred in the separated-flow region downstream of the point of strongest collapse. Interestingly, their computations did not confirm this assumption but showed that most of the energy is dissipated in the boundary layers which form on the walls *upstream* of the point of strongest collapse. Pedley & Luo (1998) attempted to employ a von Karman–Pohlhausen technique (similar to the one initially suggested by Ikeda & Matsuzaki 1999) to incorporate these findings into an improved 1D model. Unfortunately, the predictions from this model agreed only poorly with those from the 2D computations.

In a later study, Luo & Pedley (1998) showed that the inclusion of wall inertia into the system allows the wall to perform flutter-type oscillations of relatively high frequency. During the early stages of the self-excited oscillations, these higher-frequency oscillations were found to be merely superimposed on to the lower-frequency oscillations which develop in the absence of wall inertia. However, the higher-frequency oscillations were found to grow in amplitude so that they ultimately dominated the system's behaviour. Attempts were made to relate these observations to the predictions from stud-

ies of flutter-type instabilities in flows past compliant boundaries (Grotberg & Reiss 1984; Davies & Carpenter 1997*a*, 1997*b*; Larose & Grotberg 1997). Some common trends were observed but overall the agreement tended to be no more than qualitative, presumably because of the significant differences between the systems considered in the different studies (large amplitude oscillations of a finite-length elastic wall in Luo & Pedley (1998) vs. small amplitude oscillations of (usually) infinite, initially undisturbed panels in the flutter-type studies). It was established, however, that in all cases the unstable growth of the high-frequency oscillations was caused by the energy transfer from the fluid into the wall, which is possible because of the inertially-induced phase differences between the fluid loading and the wall displacement field. This behaviour is typical of a class-B flutter instability.

In all the computational studies reviewed so far, the transmural pressure at the far downstream end of the rigid tube ($p_{tm}^{(exit)} = p_{exit} - p_{ext}$ in Fig. 2) was held constant while other parameters (such as the flow rate or the wall tension) were varied. Under these conditions, an increase in the driving pressure drop, $\Delta p = p_{entry} - p_{exit}$ can be caused only by an increase in the upstream transmural pressure $p_{tm}^{(entry)} = p_{entry} - p_{ext}$ which causes the wall to bulge out. Hence the channel's flow resistance decreases as the flow rate is increased, leading to pressure-drop limitation. Physiologically more relevant is the case in which the upstream transmural pressure $p_{tm}^{(entry)}$ is held constant (corresponding to the conditions during forced expiration from the lung, for example). An increase in Δp (by lowering the downstream transmural pressure) now increases the collapse of the wall and thus increases the overall flow resistance. Luo & Pedley (2000) confirmed the expected occurrence of flow limitation in the 2D model but failed to confirm any correlation between flow limitation and the onset of self-excited oscillations. Both stable and unstable solutions were found in the flow-limited regime. The stability properties of the steady solutions were also found to be strongly dependent on the boundary conditions and in particular on the position at which pressures and fluxes were prescribed. This is consistent with the findings in Pedrizzetti's (1998) study of forced oscillations in axisymmetric collapsible tubes.

6. Three-dimensional models

The 2D physical model discussed in the previous section is a rational and (at least in principle) realisable system which can be interpreted as an approximation to the flow in a strongly collapsed 3D tube. However, it is clear that the model ignores many potentially important 3D effects such as **(i)** the strong three-dimensionality of the flow field during phases when

the tube collapse is moderate; **(ii)** the significant differences between flow separation in 2D and 3D flows (see e.g. Tobak & Peake 1982); and **(iii)** the drastic changes in wall stiffness as the tube changes from an axisymmetric to a non-axisymmetrically buckled state.

6.1. THE MODEL PROBLEM

The first step towards the development of a rational computational model of flow in 3D collapsible tubes was undertaken in Heil's (1995) PhD thesis. The collapsible tube was modelled as a thin-walled elastic shell (of length L_0, radius R_0 and wall thickness h) whose deformation was described by large-displacement, geometrically nonlinear shell theory. It is known from the experiments of, e.g., Elad *et al.* (1992) that the non-axisymmetric collapse of thin-walled elastic tubes only induces small extensional deformations of the tube wall. Therefore, a linear stress-strain relationship with two elastic constants (Young's modulus E and the Poisson ratio ν), was used as the constitutive equation.

The tube's undeformed geometry was described by the position vector $\mathbf{r}_w(\zeta^1, \zeta^2)$ to the tube's midplane which was parametrised by two Lagrangian coordinates ζ^1 and ζ^2. The vector field $\mathbf{v}(\zeta^1, \zeta^2)$ which displaces material particles to their new positions $\mathbf{R}_w = \mathbf{r}_w + \mathbf{v}$ was then determined from the principle of virtual displacements

$$\int_0^{2\pi} \int_0^{L_0/R_0} \left[E^{\alpha\beta\gamma\delta} \left(\gamma_{\alpha\beta}\ \delta\gamma_{\gamma\delta} + \frac{1}{12} \left(\frac{h}{R_0} \right)^2 \kappa_{\alpha\beta}\ \delta\kappa_{\gamma\delta} \right) - \left(\frac{R_0}{h} \right) (\mathbf{f} \cdot \delta\mathbf{R}_w) \right] d\zeta^1 d\zeta^2 = 0, \quad (18)$$

where $\gamma_{\alpha\beta}$ and $\kappa_{\alpha\beta}$ are the midplane strain and bending tensors, respectively, and $E^{\alpha\beta\gamma\delta}$ represents the fourth order tensor of elastic constants; see Heil & Pedley (1996) for details. The load vector $\mathbf{f}$ is given by the combination of the external pressure and the traction that the fluid exerts onto the tube wall. A finite-element method was used to discretise the variational equation (18).

6.2. STEADY FLOWS IN COLLAPSIBLE TUBES

In a series of papers, Heil & Pedley (1995, 1996) and Heil (1996) coupled the wall model (18) to a lubrication-theory-based description of the fluid mechanics and investigated **(i)** the flow through axisymmetric tubes, **(ii)** the tubes' linear stability to non-axisymmetric perturbations and **(iii)** their large-displacement postbuckling behaviour, respectively.

For strongly buckled tubes, the wall slope is no longer small and the applicability of lubrication theory must be questioned. Therefore, Heil (1997) replaced the lubrication-theory model by a solution of the 3D steady Stokes equations and performed extensive parameter studies to investigate the system's behaviour under conditions which correspond to typical experimental procedures. The computational study was accompanied by an experimental investigation and good agreement between the numerical predictions and the experimental results was reported. Interestingly, the predictions from the lubrication-theory model were found to agree very well with those from the full Stokes equations, even in cases where the tube was strongly collapsed.

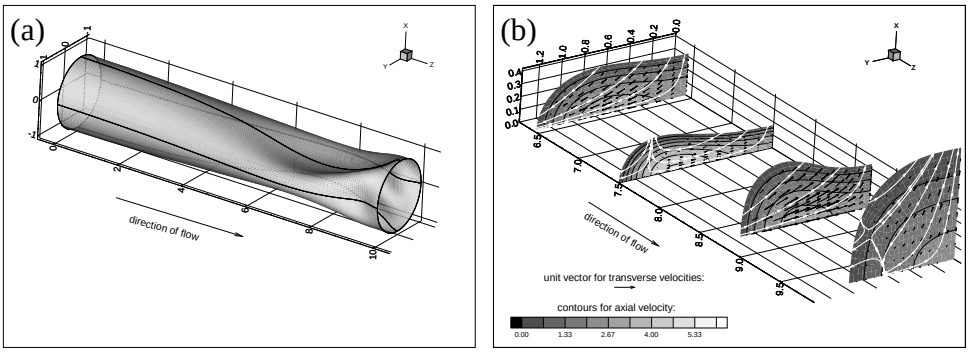

Figure 10. Strongly collapsed tube conveying viscous flow at zero Reynolds number. (a) Wall shape. (b) Flow field in four cross-sections in the most strongly collapsed part of the tube. The white lines indicate the streamlines of the transverse velocity field. After Heil & Pedley (1996).

Figure 10 illustrates the wall deformation and the flow field inside a strongly buckled elastic tube which conveys viscous fluid at zero Reynolds number. The noticeable asymmetry of the tube's deformation reflects the strong interaction between the fluid and solid mechanics. The tube's upstream end is distended by a large positive fluid pressure. In the absence of fluid inertia, the fluid pressure decreases continuously in the streamwise direction. This leads to an increasingly strong compression of the tube wall which causes the tube's downstream end to buckle strongly. The increased flow resistance in the most strongly collapsed part of the tube creates a large local pressure drop. This compresses the tube's downstream end so much that two small regions on the tube's sidewall buckle inwards, creating two 'dimples' near the horizontal plane of symmetry.

Figure 10 highlights a number of important differences between flows in collapsible channels and tubes: **(i)** The flow in the most strongly collapsed part of the tube has little resemblance to the flow between two parallel membranes. The contours of the axial velocity show that, long before the first occurrence of opposite wall contact, the axial flow begins to split up into two separate branches as it passes around the most strongly collapsed region near the tube's centreline. Recent computational studies of finite-Reynolds-number flows in collapsible tubes (Hazel & Heil 2002) confirmed the development of similar flow structures in the presence of fluid inertia. Two distinct 'jets' develop in the outer lobes when the fluid passes through the most strongly collapsed cross-section. The jets are deflected by the two 'dimples' in the sidewall and persist for a significant axial length until secondary flows and transverse diffusion of momentum smooth out the peaks in the axial velocity. The structure of the separated-flow region (consisting of a relatively passive separation bubble in the centre of the tube) was found to be fundamentally different from that observed in collapsible channels. These findings are consistent with the experimental observations of Bertram & Godbole (1997) and Moore *et al.* (1995). **(ii)** Even though the tube's upstream end is strongly pressurised, its large extensional stiffness prevents significant axisymmetric inflation; consequently very little bulging is observed. This is in line with experimental observations but is in stark contrast to the predictions from the 2D model. **(iii)** Given the wall deformation shown in Fig. 10, is not clear in what way axial tension should be represented in a tube-law-based model of the wall mechanics. The tension term in the modified tube law (10) is based on the assumption that the tensioned wall collapses radially inwards as sketched in Fig. 2. However, Fig. 10(a) shows that this assumption is only justified in the tube's vertical plane of symmetry where little flow takes place. A significant part of the tube wall (in the vicinity of the horizontal plane of symmetry) bulges radially outwards. The convex wall curvature in this region implies that axial tension would manifest itself in a relation similar to (10) but with a plus rather than a minus sign. These observations raise serious doubts as to whether it is reasonable to assume that flow in a collapsible tube is similar to flow between two parallel tensioned membranes. Furthermore, while axial tension represents an essential ingredient for the formulation of the 2D model, Heil & Pedley (1996) showed that it is only of minor importance for the deformation of 3D tubes. This observation is also consistent with experimental observations. Most investigators subject their tubes to a certain amount of axial tension, primarily to keep the tube from sagging under its own weight. Despite the fact that it is difficult to prescribe precisely the axial pre-stretch in an experiment, the tube's behaviour does not seem to

be significantly affected by this lack of control.

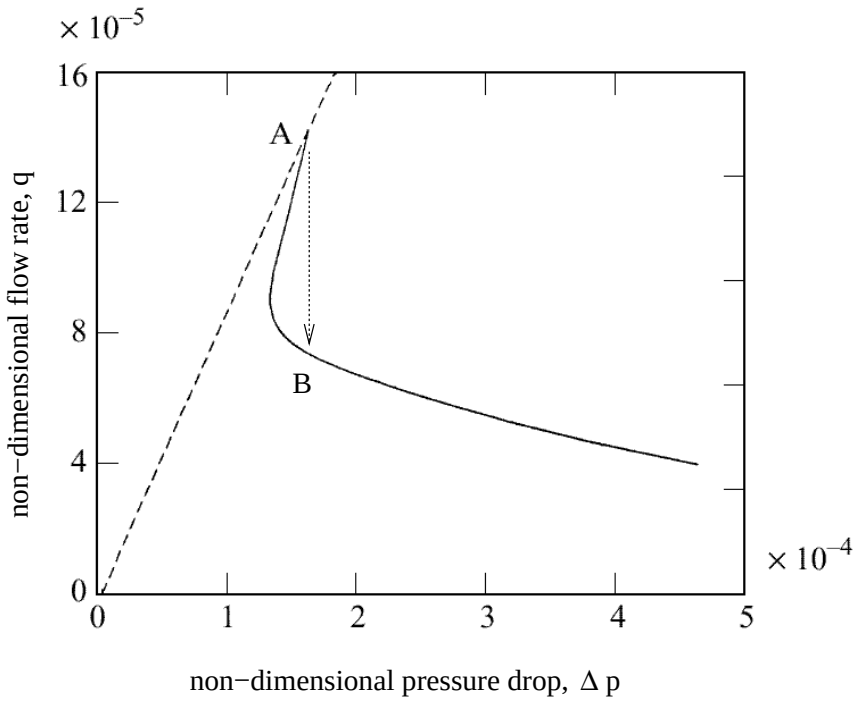

Figure 11. Volume flux as a function of the driving pressure drop through the tube for constant upstream transmural pressure $p_{tm}^{(up)} = 0$. After Heil & Pedley (1996).

Figure 11 illustrates how the nondimensional volume flux, $q = \frac{8\mu Q L_0}{\pi R_0^4 E}$, varies with the driving pressure drop, $\Delta p = (p_{up} - p_{down})/E$ when the upstream transmural pressure $p_{tm}^{(up)} = p_{up} - p_{ext}$ is held at a constant value (again with $Re = 0$). Since the flow is driven by a reduction in the downstream transmural pressure, an increase in Δp increases the compressive load on the initially axisymmetric tube. In the axisymmetric state (represented by the dashed line), the tube's deformation remains very small and the relation between flow rate and pressure drop is essentially linear. However, when the compression of the tube's downstream end exceeds a critical value (at point A), the axisymmetric state loses its stability and the tube buckles non-axisymmetrically. Fig. 11 shows that buckling occurs via a subcritical bifurcation. If the pressure drop Δp is held constant during buckling, the tube jumps dynamically to a new strongly collapsed equilib-

rium state (point B) on the post-buckled branch (represented by the solid line). In the collapsed state, the tube's flow resistance is strongly increased, and therefore the flow rate drops significantly during buckling. A further increase in the driving pressure drop leads to a further reduction in flow, illustrating the occurrence of negative effort dependence through a purely viscous mechanism.

Fig. 11 demonstrates that the transition between axisymmetric and non-axisymmetric configurations (which cannot easily be incorporated into lower dimensional models) plays a crucial role in the system's behaviour. In experimental studies, the existence of small imperfections will make the transition between axisymmetric and non-axisymmetric states less abrupt. However, Heil & Pedley's (1996) computations with a circumferentially varying external pressure showed that the system's overall behaviour is not strongly affected by the presence of such imperfections.

7. Summary and suggestions for future work

The theoretical investigations reviewed in this Chapter have provided valuable insight into the behaviour of collapsible tubes, both in laboratory experiments and in a variety of physiological applications. The detailed analyses of relatively simple 1D models have allowed the identification of a number of mechanisms which provide qualitative (and occasionally quantitative) explanations for the experimentally observed behaviour of collapsible tubes. However, almost all 1D models involve a certain number of *ad hoc* assumptions whose validity needs to be assessed critically. The analysis of self-excited oscillations in 2D collapsible channels suggests that it might be beneficial to develop improved 1D models which incorporate features such as dissipation in boundary layers and possibly the interaction between wall oscillation and vorticity waves.

The computational and asymptotic analyses of flow in 2D collapsible channels have provided much insight into the details of the complex fluid-structure interaction in this system. Our understanding could be further improved by systematic analyses of the stability of steady flows. Asymptotic approaches (similar to those employed by Guneratne 1999 and Jensen & Heil 2002) will be most appropriate for the analysis of flows in slightly deformed channels, whereas the stability of flows in strongly collapsed channels will probably have to be determined numerically. Further interaction with researchers interested in the stability of flows past compliant walls (see Chapters 4 and 5) can be expected to be particularly beneficial for the study of this problem.

Detailed numerical investigations of steady finite-Reynolds-number flows in 3D collapsible tubes are currently in progress and have already revealed

many features which cannot be predicted by any of the lower-dimensional models. The extension of such studies to unsteady flows will demand significant computational resources but would, for example, reveal whether vorticity waves, which appear to play a significant role in the large-amplitude self-excited oscillations in collapsible channels, have an equivalent (or even any) relevance in 3D flows. The development of large-Reynolds-number asymptotic analyses of flows in slightly buckled elastic tubes can be expected to provide useful insight into the structure of flow separation and the development of flow instabilities in this system.

The challenge of understanding self-excited oscillations in collapsible tubes, and in related problems involving flows over compliant surfaces, remains substantial. As the studies reviewed here have demonstrated, however, the combined use of theoretical, computational and experimental techniques can provide significant advances in areas that at first seemed intractable. We have good reason to be optimistic about significant future progress in this field.

References

AITTOKALLIO, T., GYLLENBERG, M. & POLO, O. 2001 A model of a snorer's upper airway. *Math. Biosci.* **170**, 79–90.

ARMALY, B. F., DURST, F. J., PEREIRA, C. F. & SCHONUNG, B. 1983 Experimental and theoretical investigation of backward-facing step flow. *J. Fluid Mech.* **127**, 473–496.

BALINT, T. S. 2001 Dynamics of the upper airway. PhD thesis, University of Warwick, Warwick.

BENJAMIN, T. 1963 The threefold classification for unstable disturbances in flexible surfaces bounding inviscid flows. *J. Fluid Mech.* **16**, 436–450.

BERKE, G. S., GREEN, D. C., SMITH, M. E., ARNSTEIN, D. P., HONRUBIA, V., NATIVIDAD, M. & CONRAD, W. A. 1991 Experimental-evidence in the invivo canine for the collapsible tube model of phonation. *J. Acoust. Soc. Am.* **89**, 1358–1363.

BERTRAM, C. 1986 Unstable equilibrium behavior in collapsible tubes. *J. Biomech.* **19**, 61–69.

BERTRAM, C. D. & GODBOLE, S. A. 1997 LDA measurements of velocities in a simulated collapsed tube. *ASME J. Biomech. Engng* **119**, 357–363.

BERTRAM, C. D. & PEDLEY, T. J. 1982 A mathematical model of unsteady collapsible tube behaviour. *J. Biomech.* **15**, 39–50.

BERTRAM, C. D. & RAYMOND, C. J. 1991 Measurements of wave speed and compliance in a collapsible tube during self-excited oscillations: a test of the choking hypothesis. *Med. Biol. Eng. Comput.* **29**, 493–500.

BERTRAM, C. D., RAYMOND, C. J. & BUTCHER, K. S. A. 1989 Oscillations in a collapsed-tube analog of the brachial artery under a sphygmomanometer cuff. *ASME J. Biomech. Engng* **111**, 185–191.

BERTRAM, C. D., RAYMOND, C. J. & PEDLEY, T. J. 1990 Mapping of instabilities for flow through collapsible tubes of differering length. *J. Fluids. Struct.* **4**, 125–153.

BERTRAM, C. D., RAYMOND, C. J. & PEDLEY, T. J. 1991 Application of nonlinear dynamics concepts to the analysis of self-excited oscillations of a collapsible tube conveying a fluid. *J. Fluids. Struct.* **5**, 391–426.

BINNS, R. L. & KU, D. N. 1989 Effect of stenosis on wall motion — a possible mechanism of stroke and transient ischemic attack. *Arteriosclerosis* **9**, 842–847.

BOGDANOVA, E. V. & RHYZOV, O. S. 1983 Free and induced oscillations in Poiseuille flow. *Quart. J. Mech. Appl. Math.* **36**, 271–287.

BONIS, M. & RIBREAU, C. 1978 Etude de quelques proprietes de l'ecoulement dans une conduite collabable. *La Houille Blanche* **3/4**, 165–173.

BROOK, B. S. 1997 The effect of gravity on the haemodynamics of the giraffe jugular vein. PhD thesis, University of Leeds, Leeds.

BROOK, B. S., FALLE, S. A. E. G. & PEDLEY, T. J. 1999 Numerical solutions

for unsteady gravity-driven flows in collapsible tubes: evolution and roll-wave instability of a steady state. *J. Fluid Mech.* **396**, 223–256.

BROOK, B. S. & PEDLEY, T. J. 2001 A model for time-dependent flow in (giraffe jugular) veins: Uniform tube properties. *J. Biomech.* (In print).

BROWER, R. W. & SCHOLTEN, C. 1975 Experimental evidence on the mechanism for the instability of flow in collapsible vessels. *Med. Biol. Engng* **13**, 839–845.

CAI, Z. & LUO, X. Y. 2001 A fluid-beam model for flow in collapsible channels.

CANCELLI, C. & PEDLEY, T. J. 1985 A separated-flow model for collapsible-tube oscillations. *J. Fluid Mech.* **157**, 375–404.

CAREW, E. O. & PEDLEY, T. 1997 An active membrane model for peristaltic pumping .1. Periodic activation waves in an infinite tube. *J. Biomech. Engng* **119**, 66–76.

CARPENTER, P. W., BERKOUK, K. & LUCEY, A. D. 1999 A theoretical model of pressure propagation in the human spinal CSF system. *Engineering Mechanics* **6**, 213–228.

CARPENTER, P. W., BERKOUK, K. & LUCEY, A. D. 2001*a* Pressure wave propagation in fluid-filled co-axial elastic tubes. Part 1: Basic theory. (Submitted).

CARPENTER, P. W., BERKOUK, K. & LUCEY, A. D. 2001*b* Pressure wave propagation in fluid-filled co-axial elastic tubes. Part 2: Mechanisms for the pathogenesis of syringomyelia. (Submitted).

CHANG, H.-C. & DEMEKHIN, E. A. 1996 Solitary wave formation and dynamics on falling films. *Adv. Appl. Mech.* **32**, 1–58.

CONRAD, W. A. 1969 Pressure-flow relationship in collapsible tubes. *IEEE Trans. Bio-Med. Engng* **BME-16**, 284–295.

COWLEY, S. J. 1981 High Reynolds number flows through channels and tubes. PhD thesis, University of Cambridge, Cambridge.

COWLEY, S. J. 1982 Elastic jumps on fluid-filled elastic tubes. *J. Fluid Mech.* **116**, 459–473.

COWLEY, S. J. 1983 On the wavetrains associated with elastic jumps on fluid-filled elastic tubes. *Q. J. Mech. Appl. Math.* **36**, 289–312.

DAI, G., GERTLER, J. P. & KAMM, R. D. 1999 The effects of external compression on venous blood flow and tissue deformation in the lower leg. *ASME J. Biomech. Engng* **121**, 557–564.

DANAHY, D. T. & RONAN, J. A. 1974 Cervical venous hum in patients on chronic hemodialysis. *New Eng. J. Med.* **291**, 237–239.

DAVIES, C. & CARPENTER, P. W. 1997*a* Instabilities in a plane channel flow between compliant walls. *J. Fluid Mech.* **352**, 205–243.

DAVIES, C. & CARPENTER, P. W. 1997*b* Numerical simulation of the evolution of Tollmien-Schlichting waves over finite compliant panels. *J. Fluid Mech.* **335**, 361–392.

DAWSON, S. V. & ELLIOT, E. A. 1977 Wave-speed limitation on expiratory flow – a unifying concept. *J. Appl. Physiol.* **43**, 498–515.

DRESSLER, R. F. 1949 Mathematical solution of the problem of roll-waves in inclined open channels. *Commun. Pure Appl. Math.* **2**, 149–194.

ELAD, D., KAMM, R. D. & SHAPIRO, A. H. 1987 Choking phenomena in a lung-like model. *ASME J. Biomech. Engng* **109**, 1–9.

ELAD, D., SAHAR, M., AVIDOR, J. M. & EINAV, S. 1992 Steady flow through collapsible tubes: measurements of flow and geometry. *ASME J. Biomech.*

Engng **114**, 84–91.

ELLIOT, E. A. & DAWSON, S. V. 1977 Test of wave-speed theory of flow limitation in elastic tubes. *J. Appl. Physiol.* **43**, 516–522.

FEE, M. S., SHRAIMAN, B., PESARAN, B. & MITRA, P. 1998 The role of nonlinear dynamics of the syrinx in the vocalizations of a songbird. *Nature* **395**, 67–71.

FLAHERTY, J. E., KELLER, J. B. & RUBINOW, S. I. 1972 Post buckling behavior of elastic tubes and rings with opposite sides in contact. *SIAM J. Appl. Math.* **23**, 446–455.

GAVRIELY, N. & JENSEN, O. E. 1993 Theory and measurements of snores. *J. Appl. Physiol.* **74**, 2828–2837.

GAVRIELY, N., PALTI, Y., ALROY, G. & GROTBERG, J. B. 1984 Measurement and theory of wheezing breath sounds. *J. Appl. Physiol.* **57**, 481–492.

GAVRIELY, N., SHEE, T. R., CUGELL, D. W. & GROTBERG, J. B. 1989 Flutter in flow-limited collapsible tubes: a mechanism for the generation of wheezes. *J. Appl. Physiol.* **66**, 2251–2261.

GREGG, D. E. & FISHER, L. C. 1963 Blood supply to the heart. In *Handbook of Physiology* (ed. W. F. Hamilton & P. Dow). Section 2: Circulation, Volume II. Washington D. C.: American Physiological Society.

GRIFFITHS, D. J. 1969 Urethral elasticity and micturition hydrodynamics in females. *Med. Biol. Engng Comput.* **7**, 201–215.

GRIFFITHS, D. J. 1971 Hydrodynamics of male micturition – I: Theory of steady flow through elastic-walled tubes. *Med. Biol. Engng Comput.* **9**, 581–588.

GROTBERG, J. B. 1994 Pulmonary flow and transport phenomena. *Ann. Rev. Fluid Mech.* **26**, 529–571.

GROTBERG, J. B. & DAVIS, S. H. 1980 Fluid-dynamical flapping of a collapsible channel: sound generation and flow limitation. *J. Biomech.* **13**, 219–230.

GROTBERG, J. B. & REISS, E. L. 1984 Subsonic flapping flutter. *Journal of Sound and Vibration* **92**, 349–361.

GROTBERG, J. B. & SHEE, T. R. 1985 Compressible-flow channel flutter. *J. Fluid Mech.* **159**, 175–193.

GUIOT, C., PIANTA, P. G., CANCELLI, C. & PEDLEY, T. J. 1990 Prediction of coronary blood-flow with a numerical-model based on collapsible tube dynamics. *Am. J. Physiol.* **258**, H1606–H1614.

GUNERATNE, J. C. 1999 High-Reynolds number flow in a collapsible channel. PhD thesis, Cambridge University, Cambridge.

GUNERATNE, J. C. & PEDLEY, T. J. 2001 High Reynolds number flow in a collapsible channel. (In preparation).

HAYASHI, S., HAZASE, T. & KAWAMURA, H. 1998 Numerical analysis for stability and self-excited oscillation in collapsible tube flow. *ASME J. Biomech. Engng* **120**, 468–475.

HAZEL, A. L. & HEIL, M. 2002 Steady finite Reynolds number flow in collapsible tubes. (In preparation). See also `http://www.cse.clrc.ac.uk/Coordination/Biofluids/Talks/mheil.pdf`.

HEIL, M. 1995 Large deformations of cylindrical shells conveying viscous flow. PhD thesis, University of Leeds, Leeds.

HEIL, M. 1996 The stability of cylindrical shells conveying viscous flow. *J. Fluids. Struct.* **10**, 173–196.

HEIL, M. 1997 Stokes flow in collapsible tubes: computation and experiment. *J.*

Fluid Mech. **353**, 285–312.

HEIL, M. & PEDLEY, T. J. 1995 Large axisymmetric deformations of cylindrical shells conveying viscous flow. *J. Fluids. Struct.* **9**, 237–256.

HEIL, M. & PEDLEY, T. J. 1996 Large post-buckling deformations of cylindrical shells conveying viscous flow. *J. Fluids. Struct.* **10**, 565–599.

HUANG, L. 1995 Flutter of cantilevered plates in axial flow. *J. Fluids Struct.* **9**, 127–147.

HUANG, L. 1998 Reversal of the Bernoulli effect and channel flutter. *J. Fluids. Struct.* **12**, 131–151.

HUANG, L. 2001 Viscous flutter of a finite elastic membrane in Poiseuille flow. *J. Fluids Struct.* **15**, 1060–1088.

IKEDA, T. & MATSUZAKI, Y. 1999 A one-dimensional unsteady separable and reattachable flow model for collapsible tube-flow analysis. *ASME J. Biomech. Engng* **121**, 153–159.

JENSEN, O. E. 1990 Instabilities of flow in a collapsed tube. *J. Fluid Mech.* **220**, 623–659.

JENSEN, O. E. 1992 Chaotic oscillations in a simple collapsible-tube model. *ASME J. Biomech. Engng* **114**, 55–59.

JENSEN, O. E. 1998 An asymptotic model of viscous flow limitation in a highly collapsed channel. *ASME J. Biomech. Engng* **120**, 544–547.

JENSEN, O. E. 2001 Self-excited oscillations in a collapsible channel: insights from a simple asymptotic model. (preprint).

JENSEN, O. E. & HEIL, M. 2002 Self-excited oscillations in a collapsible channel. (In preparation).

JENSEN, O. E. & PEDLEY, T. J. 1989 The existence of steady flow in a collapsed tube. *J. Fluid Mech.* **206**, 339–374.

KAMM, R. D. 1982 Bioengineering studies of periodic external compression as prophylaxis against deep vein thrombosis – Part I: numerical studies. *ASME J. Biomech. Engng* **104**, 87–95.

KAMM, R. D. & PEDLEY, T. J. 1989 Flow in collapsible tubes: a brief review. *ASME J. Biomech. Engng* **111**, 177–179.

KAMM, R. D. & SHAPIRO, A. H. 1979 Unsteady flow in a collapsible tube subjected to external pressure or body forces. *J. Fluid Mech.* **95**, 1–78.

KATZ, A. I., CHEN, Y. & MORENO, A. H. 1969 Flow through a collapsible tube – experimental analysis and mathematical model. *Biophys. J.* **9**, 1261–1279.

KECECIOGLU, I., MCCLURKEN, M. E., KAMM, R. D. & SHAPIRO, A. H. 1981 Steady, supercritical flow in collapsible tubes. Part 1. Experimental observations. *J. Fluid Mech.* **109**, 367–389.

KISTLER, S. F. & SCRIVEN, L. E. 1983 Coating flows. In *Computational Analysis of Polymer Processing* (ed. J. Pearson & S. Richardson). London: Applied Science Publishers.

KU, D. N. 1997 Blood flow in arteries. *Ann. Rev. Fluid Mech.* **29**, 399–434.

LANDAHL, M. 1962 On the stability of a laminar incompressible bounadry layer over a flexible surface. *J Fluid. Mech.* **13**, 607–632.

LAROSE, P. G. & GROTBERG, J. B. 1997 Flutter and long-wave instabilities in compliant channels conveying developing flows. *J. Fluid Mech.* **331**, 37–58.

LIANG, S.-J., NEITZEL, G. P. & AIDUN, C. K. 1997 Finite element computations for unsteady fluid and elastic membrane interaction problems. *Int. J. Num. Meth. Fluids* **24**, 1091–1110.

LIGHTHILL, J. 1975 *Mathematical biofluiddynamics*. Philadelphia: SIAM.

LOWE, T. W. & PEDLEY, T. J. 1995 Computation of Stokes flow in a channel with a collapsible segment. *J. Fluids. Struct.* **9**, 885–905.

LUO, X. Y. & PEDLEY, T. J. 1995 Numerical simulation of steady flow in a 2-d collapsible channel. *J. Fluids. Struct.* **9**, 149–197.

LUO, X. Y. & PEDLEY, T. J. 1996 A numerical simulation of unsteady flow in a two-dimensional collapsible channel. *J. Fluid Mech.* **314**, 191–225.

LUO, X. Y. & PEDLEY, T. J. 1998 The effects of wall inertia on flow in a two-dimensional collapsible channel. *J. Fluid Mech.* **363**, 253–280.

LUO, X. Y. & PEDLEY, T. J. 2000 Multiple solutions and flow limitation in collapsible channel flows. *J. Fluid Mech.* **420**, 301–324.

MATSUZAKI, Y. & FUJIMURA, K. 1995 Reexamination of steady solutions of a collapsible channel conveying fluid. *ASME J. Biomech. Engng* **117**, 492–494.

MATSUZAKI, Y. & FUNG, Y. 1977 Stability analysis of straight and buckled two-dimensional channels conveying an incopmressible flow. *Trans. ASME E: J. Appl. Mech.* **44**, 548–552.

MATSUZAKI, Y., IKEDA, T., KITAGAWA, T. & SAKATA, S. 1994 Analysis of flow in a two-dimensional collapsible channel using universal "tube" law. *ASME J. Biomech. Engng* **116**, 469–476.

MATSUZAKI, Y. & MATSUMOTO, T. 1989 Flow in two-dimensional collapsible channel with rigid inlet and outlet. *ASME J. Biomech. Engng* **111**, 180–184.

MCCLURKEN, M. E., KECECIOGLU, I., KAMM, R. D. & SHAPIRO, A. H. 1981 Steady, supercritical flow in collapsible tubes. Part 2. Theoretical studies. *J. Fluid Mech.* **109**, 391–415.

MCDONALD, D. A. 1974 *Blood flow in arteries*, 2nd edn. London: Edward Arnold.

MOORE, J. E., STERGIOPULOS, N., GOLAY, X., KU, D. N. & MEISTER, J.-J. 1995 Flow measurements in collapsed stenotic arterial models. In *Proceedings of the 1995 Bioengineering Conference* (ed. R. M. Hochmuth, N. A. Langrana & M. S. Hefzy), , vol. ASME-BED 29, pp. 229–230.

OATES, G. C. 1975 Fluid flow in soft-walled tubes: I. Steady flow. *Med. Biol. Engng* **13**, 773–778.

OLSON, D. A., KAMM, R. D. & SHAPIRO, A. H. 1982 Bioengineering studies of periodic external compression as prophylaxis against deep vein thrombosis – Part II: experimental studies on a simulated leg. *ASME J. Biomech. Engng* **104**, 96–104.

PEDLEY, T. J. 1980 *The fluid mechanics of large blood vessels*. Cambridge: Cambridge University Press.

PEDLEY, T. J. 1992 Longitudinal tension variation in collapsible channels: A new mechanism for the breakdown of steady flow. *ASME J. Biomech. Engng* **114**, 60–67.

PEDLEY, T. J., BROOK, B. S. & SEYMOUR, R. S. 1996 Blood pressure and flow rate in the giraffe jugular vein. *Phil. Trans. Roy. Soc. London* **B 351**, 855–866.

PEDLEY, T. J. & LUO, X. Y. 1998 Modelling flow and oscillations in collapsible tubes. *Theoret. Comput. Fluid Dyn.* **10**, 277–294.

PEDLEY, T. J. & STEPHANOFF, K. D. 1985 Flow along a channel with a time-dependent indentation in one wall: the generation of vorticity waves. *J. Fluid Mech.* **160**, 337–367.

PEDRIZZETTI, G. 1998 Fluid flow in a tube with an elastic membrane insertion. *J. Fluid Mech.* **375**, 39–64.

RALPH, M. E. & PEDLEY, T. J. 1988 Flow in a channel with a moving indentation. *J. Fluid Mech.* **190**, 87–112.

RALPH, M. E. & PEDLEY, T. J. 1989 Viscous and inviscid flow in a channel with a moving indentation. *J. Fluid Mech.* **209**, 543–566.

RALPH, M. E. & PEDLEY, T. J. 1990 Flow in a channel with a moving indentation in one wall. *ASME J. Fluids Engng* **112**, 468–475.

RAST, M. P. 1994 Simultaneous solution of the Navier-Stokes and elastic membrane equations by a finite-element method. *Int. J. Num. Meth. Fluids* **19**, 1115 – 1135.

REYN, J. W. 1987 Multiple solutions and flow limitation for steady flow through a collapsible tube held open at the ends. *J. Fluid Mech.* **174**, 467–493.

RODBARD, S. 1966 A hydrodynamics mechanism for autoregulation of flow. *Cardiologia* **48**, 532–535.

RODBARD, S. & TAKACS, L. 1966 Hydrodynamics of autoregulation. *Cardiologia* **48**, 433–440.

ROSENFELD, M. 1995 A numerical study of pulsating flow behind a constriction. *J. Fluid Mech.* **301**, 203–223.

ROTHMAYER, A. P. 1989 The viscous flow through symmetric collapsible channels. *Mathematika* **36**, 153–181.

SHAPIRO, A. H. 1977 Steady flow in collapsible tubes. *ASME J. Biomech. Engng* **99**, 126–147.

SHIMIZU, M. & TANIDA, Y. 1983 On the mechanism of Korotkoff sound generation at diastole. *J. Fluid Mech.* **127**, 315–339.

SMITH, F. T. 1976*a* Flow through constricted or dilated pipes and channels. Part 1. *Q. J. Mech. Appl. Math.* **21**, 343–364.

SMITH, F. T. 1976*b* Flow through constricted or dilated pipes and channels. Part 2. *Q. J. Mech. Appl. Math.* **21**, 365–379.

SMITH, F. T. & BURGGRAF, O. R. 1985 On the development of large-sized short-scaled disturbances in boundary layers. *Proc. Roy. Soc. London A* **399**, 25–55.

SOBEY, I. 1985 Observations of waves during oscillatory channel flow. *J. Fluid Mech.* **151**, 395–426.

STEPHANOFF, K. D., PEDLEY, T. J., LAWRENCE, C. J. & SECOMB, T. W. 1983 Fluid flow along a channel with an asymmetric oscillating constriction. *Nature* pp. 692–695.

TOBAK, M. & PEAKE, D. J. 1982 Topology of three-dimensional separated flows. *Ann. Rev. Fluid Mech.* **14**, 61–85.

TSUJI, T., NAKAJIM, K., TAKEUCHI, Y., INOUE, K., SHIOMA, K., KOYAMA, Y., TOKUCHI, K., YOSHIKAWA, T. & SUMA, K. 1978 Study on haemodynamics during cardiopulmonary bypass (in Japanese). *Artificial Organs* **7**, 435–438.

TUTTY, O. 1984 High-Reynolds-number viscous flow in collapsible tubes. *J. Fluid Mech.* **146**, 451–469.

TUTTY, O. R. 1992 Pulsatile flow in a constricted channel. *ASME J. Biomech. Engng* **114**, 50–54.

TUTTY, O. R. & PEDLEY, T. J. 1993 Oscillatory flow in a stepped channel. *J. Fluid Mech.* **247**, 179–204.

UR, A. & GORDON, M. 1970 Origin of Korotkoff sounds. *American Journal of Physiology* **218**, 524–529.

WALSH, C. 1995 Flutter in one-dimensional collapsible tubes. *J. Fluids. Struct.* **9**, 393–408.

WALSH, C., SULLIVAN, P. & HANSON, J. 1991 Subcritical flutter in collapsible tube flow: a model of expiratory flow in the trachea. *J. Biomech. Engng* **113**, 21–26.

WEAVER, D. & PAÏDOUSSIS, M. 1977 On the collapse and flutter phenomena in thin tubes conveying fluid. *J. Sound Vib.* **50**, 117–132.